Maritime decarbonization pathways: a trade-off between operational and technical measures

Guewen HESLAN *

October 2024

Contents

*LEMNA, Nantes Univesité

1 Introduction

The maritime shipping industry is a fundamental component of international trade, serving as the primary conduit for the movement of goods across the world's oceans. Its significance in the global economy cannot be overstated; over 90% of the world's trade by volume is transported by sea (OECD, 2022). Containerized merchandise accounted for 15% of the total cargo mass loaded in 2022, or 26% of the dry cargo mass, and its share continues to grow (UNCTAD, 2023). Globally, seaborne trade has been increasing annually, with a 1.2% rise in 2023 (UNCTAD, 2023). Despite the efficiency of maritime shipping, which is recognized as the most energy-efficient method of transporting goods, it contributes to over 3% of global greenhouse gas (GHG) emissions (UNCTAD, 2023). Projections indicate that these emissions could increase to 130% of 2008 levels by 2050 (Faber et al., 2021). Containerships are responsible of about 26% of total maritime shipping GHG emissions (OECD, 2023). To address this concern, multiple international actors introduced carbon emissions policies as IMO, whose member states have adopted energy efficiency measures program to reduce the carbon intensity of international shipping by 40% in 2030 compared to 2008 through EEDI (Energy Efficiency Design Index) for more efficient new ships, SEEMP (Ship Energy Efficiency Management Plan) for operational measures and EEXI (Energy Efficiency Existing Ship Index) for existing ships measures (IMO, 2024). The European Union has also introduced objectives in the reducing of carbon emissions with FuelEU which aims to increase the demand for renewable and low carbon fuels. In another way, EU enlarged the Emissions Trading Scheme to maritime shipping in early 2024 with a planned gradual extension to new types of vessel (EU Council, 2023). Market based measures as carbon pricing are already being implemented in maritime shipping and will have effects on maritime actor's strategies.

Given that containerships represent a significant contributor to maritime shipping GHG emissions, we have chosen to focus our attention on this particular market segment in order to gain insight into the potential responses of shipowners to the introduction of carbon pricing. The strategy employed by containerships firms has been the subject of extensive analysis in the academic literature, with a particular focus on liner companies, which represent the core element of containership utilisation. The specific characteristics of liner shipping companies make it easier to model them: routes are already established and change little over the years (Corbett et al., 2009), prices fluctuate less than spot prices because of the long-term contracts established between traders and shipowners, thus the quantities transported are less subject to fluctuations. Liner Shipping Fleet Deployment (LSFD) problem literature address most strategy decisions of liner company though disaggregated cost structure using cost minimization. It understands scheduling, vessel deployment, cargo-handling operations. LSFD literature is based on 7 major assumptions : port rotations are given, fleet is given and classified into different types homogeneous in characteristics as capacity and cost structure, demand is exogeneous and is independent of factors as transit time and freight rate, ports can provide service whenever a ship arrives, containers transported are modelized as a continuous variable, ships can immediately serve any port rotations, and bunker price, port charges, freight rate are known (Wang and Meng, 2017). Since LSFD literature is large and long-standing (Perakis and Jaramillo, 1991; Jaramillo and Perakis, 1991), many extension have been explored as transhipment, sailing speed optimization, etc. An abundant literature has developed around the issue of fleet deployment and its impact on the environment (Kontovas, 2014). Zhu et al. (2018) evaluate the effect of maritime ETS on fleet composition, by varying the price of CO2, their results demonstrate an incentive to use new technologies and deploy more energy-efficient ships when METS is deployed. Gu et al. (2019) estimate the effect of maritime ETS at a regional and global scale, looking at the impact on fleet operations.

It is commonly assumed that there are two ways to reduce shipping emissions: an operational way through fleet operation management and a technical way through technological measures as reflected by both IMO policies EEDI/EEXI and SEEMP. IMO suggested some options : enlargement of vessel size, reduction of voyage speed and application of new technology (Woo and Moon, 2014). Speed control is considered as one of the most efficient emission-mitigation measure (Nepomuceno de

Oliveira et al., 2022). Carbon emissions are directly proportional to fuel consumption, which increases as sailing speed increases. According to Faber et al. (2011), a 10% speed reduction would lead to 19% fuel savings, more recent IMO results give a 7.38% reduction potential for a 10% speed decrease, and 12.60% for 20% speed decrease (Faber et al., 2021). According to literature, speed reduction could represent an effective short-run adaptation (Corbett et al., 2009). Slow-steaming, as reduced speed is called, has already been adopted by shipowners, notably in late 2000s with high fuel prices (Cariou, 2011). Many studies assessed the effect of speed reduction on fuel consumption and then carbon emissions associated (Norlund and Gribkovskaia, 2013; Woo and Moon, 2014; Cepeda et al., 2017). Corbett et al. (2009) estimate the cost-effectiveness of speed reduction and obtain a 20-30% speed reduction under a 150$/ton fuel tax while while Taskar and Andersen (2020) obtain that a 30% speed reduction leads to varying fuel savings from 2% to 45% depending on ship characteristics. Lindstad et al. (2011) investigate the effect of speed reduction on direct emissions, they obtain a 19% emission reduction keeping a negative abatement cost. If it is commonly assumed that sailing speed is given (Shintani et al., 2007; Wang and Meng, 2012), a significant part of the LSFD literature has focused on fleet deployment problems, considering the speed at which the boats are sailing. Perakis and Jaramillo (1991) have laid the foundations of CLFD (Container Liner Fleet Deployment) model representing operating cost of liner ships using speed optimization. The optimal speed is determined by annual operating cost minimization. More recent literature keep proposing sailing speed optimisation using more complex fuel consumption function form (Gelareh and Meng, 2010; Xia et al., 2015). One of the common forms is the cubic-law which is a non-linear form representing the exponential consumption resulting from speed rising with some limits (Adland et al., 2020; Kristensen, 2012).

If speed reduction seems an interesting way to reduce carbon emissions, limitations must be taken into account when considering the applicability of this approach. First, if LSFD assume a complete availability of ports, in facts there is an actual lack of flexibility in scheduling, especially with established contracts. Second, given the fairly stable demand, the addition of new vessels to the fleet seems necessary to support a similar flow of goods. As Taskar and Andersen (2020) points out, "speed reduction can lead to an increase in the number of ships to fulfill the transport demand". Corbett et al. (2009) consider two scenarios, with and without additional ships. Emission decrease is bigger when no additional ship is introduced but marginal costs are higher than usually reported due to lost profit from reduced service. Norlund and Gribkovskaia (2013); Psaraftis and Kontovas (2010) admit that low sailing speed results in increasing fleet size and higher costs. For the second, the introduction of technical carbon abatement measures seems necessary to reduce efficiently shipping carbon emissions.

Literature on technical measures in the maritime shipping sector can be divided into two main parts. A major part focus on Marginal Abatement Cost (MAC) estimation. Faber et al. (2011) propose a review of carbon abatement measures for several measures, estimation carbon abatement potential, recuring cost as CAPEX, non-recuring cost as OPEX. Yuan et al. (2016) propose a method to quantify uncertainty in emissions reduction, estimation stochastic marginal abatement cost through carbon abatement potential lower and upper bound for each measure. From expert based, company and bottom-up data, Irena et al. (2021) gives MACC for a set of several measures from CAPEX, OPEX and abatement potential. From this, they propose a ranking of measures, with some permitting negative marginal abatement costs. Since IMO has set Emission Control Aeras for air pollutant, a literature has developed on the effect of these policy aeras on fleet manager strategies. Zhen et al. (2020) propose a decision-making fleet deployment class model for ECA specific-measures investment decision through a mixed integer programming model. As most recent common LSFD model, the cost is minimised to obtain optimal sailing speed, cargo allocation. In their model, measure investment decision are essential as if they do not adopt them, the operating cost will increase. Ren and Lützen (2015) propose a decision making method for pollutant emission-reduction technology , they consider 9 criteria as maturity, costs, environmental and social aspects. Schwartz et al. (2020) focuses on CO2 emission reduction in shipping, considering investment in carbon abatement measures. They obtain that over 50% of emissions can be reduced with profitable investments using cargo cost-representation in short-sea shipping sector.

2 Problem description

The IMO has proposed two solutions for decarbonisation, but there are real limits to their practical application. The timelines for implementation differ between operational and technological measures. On the one hand, operational measures such as speed management and fleet deployment can be implemented in the short term as they don't directly require significant investment. However, these measures face constraints, especially in ports, that prevent their full implementation. Full implementation would require a reconfiguration of the relationship between shipowners and ports. Furthermore, as some authors have pointed out, managing a fleet with the aim of decarbonisation could potentially lead to an increase in the size of the fleet. This in turn would significantly increase the costs associated with investment, management and maintenance of the additional ships. On the other hand, the implementation of technological measures hinges on factors external to the management of shipowner firms. The selection of technical solutions depends on factors such as the maturity of the chosen technology, initial investment costs, and ongoing operational expenses incurred over the technology's lifecycle. Among technical solutions, energy consumption reduction measures and fuel change measures present a range of advantages and disadvantages. Energy-saving measures require reasonable investment with, for most, minimal port infrastructure but also recurring expenses. Nevertheless, the cost-effectiveness, maturity, and accessibility of these measures are heavily influenced by research and development, an area where smaller shipowners have limited influence. Fuel switching measures require the establishment of a complete fuel value chain, including port refuelling infrastructures tailored to different types of fuel conditioning. For shipowners, opting for these measures implies significant investments, which are compounded by potentially higher fuel costs compared to conventional fuels.

Taking all these parameters into account, it is important to understand the shipowner's strategy for reducing GHG emissions. The differences among these types of measures undeniably create both efficiency and temporal trade-off. The aim of this paper is to shed light on this trade-off by examining the optimal strategy of a shipowner when faced with a carbon price, and how this affects the firm's operational and investment decisions.

3 Methodology

3.1 General

We consider a liner container shipping firm operating on multiple routes with vessels of varying capacities, consistent with the literature on Liner Shipping Fleet Deployment (Wang and Meng, 2017). Our model aims to minimise the firm's total discounted cost over t^{max} periods with $t \in \mathcal{T}$, $\mathcal{T} = \{0, ..., t^{max}\}$ and determines the optimal fleet operator decisions—such as the number of vessels, speed, and carbon abatement measures—to meet port-pair demand at given carbon prices.

Routes are indexed by r within the set of routes $\mathcal{R}$ and are assumed to remain unchanged over time due to their pre-existing geographical optimisation. Each route r involves N_r stop-calls, using a route-specific leg set $i \in \mathcal{I}_r$, where $\mathcal{I}_r = \{0, 1, 2, ..., N_r\}$ and $N_r \in \mathbb{N}^*$. We denote ports by $p, o, d \in \mathcal{P}$, with $p_{r,i}$ representing the arrival port of leg i on route r. The operating fleet comprises different vessel types indexed by v in the vessel type set $\mathcal{V}$, with a subset $\mathcal{V}_r \subset \mathcal{V}$ specifying the vessel types accepted on route r. Each vessel type is defined by specific characteristics, including capacity. The methodology focuses on minimising the total discounted firm's cost while maintaining supply-demand equilibrium.

3.2 Cargo flow

Annual demand is denoted by $D_{o,d,t}$, specific to each port pair $(o, d) \in \mathcal{W}$, where $\mathcal{W} \subset \mathcal{P} \times \mathcal{P}$ represents the set of possible port pairs. We employ an "origin-link-based fleet deployment model" for cargo flow (Wang and Meng, 2017; Herrera Rodriguez et al., 2022). Let $fl_{o,r,v,i,t}$ denote the flow of goods originating from o at leg i on a type v vessel sailing on route r during year t. This model considers the dynamics of cargo flow (1), accounting for the loaded cargo $lo_{o,r,v,i,t}$ and the discharged cargo $di_{o,r,v,i,t}$. We define (2) to allow a complete loop.

$$\sum_{v \in \mathcal{V}} \left(fl_{o,r,v,i-1,t} + lo_{o,r,v,i,t} - di_{o,r,v,i,t} \right) = \sum_{v \in \mathcal{V}} fl_{o,r,v,i,t} \qquad \forall o \in \mathcal{P}, \forall r \in \mathcal{R}, \forall i \in \mathcal{I}_r, \forall t \in \mathcal{T} \tag{1}$$

$$\sum_{v \in \mathcal{V}} \left(fl_{o,r,v,N_r,t} + lo_{o,r,v,0,t} - di_{o,r,v,0,t} \right) = \sum_{v \in \mathcal{V}} fl_{o,r,v,0,t} \qquad \forall o \in \mathcal{P}, \forall r \in \mathcal{R}, \forall t \in \mathcal{T} \tag{2}$$

The total flow of containers at leg i on a type v vessel sailing on route r is constrained by the maximum capacity cap_v of the vessel type (3). Cargo fulfilled demand is denoted $df_{o,d,v,t}$ and follow the dynamics of equation (4). We considering the total annual pair-port demand $D_{o,d,t}$ (5).

$$\sum_{o \in \mathcal{P}} fl_{o,r,v,i,t} \leq cap_v \qquad \forall r \in \mathcal{R}, \forall v \in \mathcal{V}_r, \forall i \in \mathcal{I}_r, \forall t \in \mathcal{T} \tag{3}$$

$$\sum_{r \in \mathcal{R}} \sum_{\substack{i \in \mathcal{I}_r \\ p_{r,i} = d}} \phi_{r,t} m_{r,v,t} (lo_{o,r,v,i,t} - di_{o,r,v,i,t}) = df_{o,d,v,t} \qquad d \neq o, \forall (o,d) \in \mathcal{W}, \forall v \in \mathcal{V}, \forall t \in \mathcal{T} \tag{4}$$

$$\sum_{v \in \mathcal{V}} df_{o,d,v,t} = D_{o,d,t} \qquad \forall (o,d) \in \mathcal{W}, \forall t \in \mathcal{T} \tag{5}$$

At each port p, we define $lo_{p,v,t}$, $di_{p,v,t}$, and $tr_{p,v,t}$ as the cargo loaded (6), discharged (7), and transshipped (8), respectively.

$$lo_{p,v,t} = \sum_{d \in \mathcal{P}} df_{p,d,v,t} \qquad \forall p \in \mathcal{P}, \forall v \in \mathcal{V}, \forall t \in \mathcal{T} \tag{6}$$

$$di_{p,v,t} = \sum_{o \in \mathcal{P}} df_{o,p,v,t} \qquad \forall p \in \mathcal{P}, \forall v \in \mathcal{V}, \forall t \in \mathcal{T} \tag{7}$$

$$tr_{p,v,t} = \sum_{r \in \mathcal{R}} \sum_{\substack{i \in \mathcal{I}_r \\ p_{r,i}=p}} \sum_{o \in \mathcal{P}} lo_{o,r,v,i,t} - lo_{p,v,t} \qquad \forall p \in \mathcal{P}, \forall v \in \mathcal{V}, \forall t \in \mathcal{T} \tag{8}$$

3.3 Time

The total voyage time on leg i of route r is denoted $t^{tot}_{r,i,t}$ (9), comprising sailing time $t^{sea}_{r,i,t}$ (10) determined by the average speed $s_{r,t}$ and leg distance $d_{r,i,t}$. We also consider manoeuvring time $t^{man}_{r,i,t}$, berthing time $t^{ber}_{r,i,t}$ (11), using vessel-type specific parameters tp^{ber}_v (TEU/h) and canal time $t^{canal}_{r,i}$ if there is one in $i \to i+1$ leg . The total round-trip time enables computation of the number of round-trips per year ϕ_r (12).

$$t^{tot}_{r,i,t} = t^{sea}_{r,i,t} + t^{man}_{r,i,t} + t^{ber}_{r,i,t} + t^{canal}_{r,i} \qquad \forall r \in \mathcal{R}, \forall i \in \mathcal{I}_r, \forall t \in \mathcal{T} \tag{9}$$

$$t^{sea}_{r,i,t} = \frac{d_{r,i}}{s_{r,t}} \qquad \forall r \in \mathcal{R}, \forall i \in \mathcal{I}_r, \forall t \in \mathcal{T} \tag{10}$$

$$t^{ber}_{r,i,t} = \max_v \left(\sum_{o \in \mathcal{P}} \left[lo_{o,r,v,i,t} + di_{o,r,v,i,t} \right] tp^{ber}_v \right) \qquad \forall r \in \mathcal{R}, \forall i \in \mathcal{I}_r, \forall t \in \mathcal{T} \tag{11}$$

$$\phi_{r,t} = \frac{365 * 24}{\sum_{i \in \mathcal{I}_r} t^{tot}_{r,i,t}} \qquad \forall r \in \mathcal{R}, \forall t \in \mathcal{T} \tag{12}$$

We establish $m_{r,v,t}$ as the number of vessels by route and type, with $m^0_{r,v}$ representing the base number from data.

3.4 Fuel consumption

Fuel consumption, a major operating cost (Stopford, 2010), is divided between the main and auxiliary engines as Cariou et al. (2019). Main engine fuel consumption follows a cubic law (Notteboom and Cariou, 2009; Corbett et al., 2009; Wang et al., 2015; Adland et al., 2020; Cariou et al., 2023). Using Cariou et al. (2019) method, we compute cubic law from sea margin[1] sm, specific fuel consumption $SFC_{r,v,f}$, main engine power P^{me}_v and the cube of the ratio speed/vessel design speed $\frac{s_{r,t}}{s^{ds}_v}$. Authors specifies cubic law for hourly consumption as equation (13).

$$fc_{r,v,f,t} = sm * SFC_{r,v,f,t} * P^{me}_v * \left(\frac{s_{r,t}}{s^D_v} \right)^3 \qquad \forall r \in \mathcal{R}, \forall v \in \mathcal{V}_r, \forall f \in \mathcal{F}_v, \forall t \in \mathcal{T} \tag{13}$$

According to Faber et al. (2021), Specific Fuel Consumption is dependant from engine load as in equation (14).

$$SFC = SFC^{Base} * \left(0.455 * Load^2 - 0.71 * Load + 1.28\right) \tag{14}$$

[1] Refers to the impact of sea conditions on vessel consumption

As cubic law set the main engine power output $P_{r,v}^{Output}$ dependant on the cube of speed-speed design ratio $\frac{s_r}{s_v^{Design}}$ and the main engine power, we have equation (15) and so we define $SFC_{r,v}$ as a function of speed in equation (18).

$$P_{r,v,t}^{Output} = P_v^{me} * \left(\frac{s_{r,t}}{s_v^{Design}}\right)^3 \tag{15}$$

$$\Leftrightarrow \frac{P_{r,v,t}^{Output}}{P_v^{me}} = \left(\frac{s_{r,t}}{s_v^{Design}}\right)^3 \tag{16}$$

$$\Leftrightarrow Load_{r,v,t} = \left(\frac{s_{r,t}}{s_v^{Design}}\right)^3 \tag{17}$$

$$SFC_{r,v,f,t} = SFC_f^{Base} * \left(0.455 * \left(\frac{s_r}{s_v^{Design}}\right)^6 - 0.71 * \left(\frac{s_r}{s_v^{Design}}\right)^3 + 1.28\right) \qquad \forall r \in \mathcal{R}, \forall v \in \mathcal{V}_r, \forall f \in \mathcal{F}_v, \forall t \in \mathcal{T} \tag{18}$$

We consider a cubic law variable $\lambda_{r,v,f}$ to make cubic law more explicit (19). From this we compute sailing main engine consumption $fc_{r,i,v,f,t}^{me}$ for $i-1 \longrightarrow i$ trip on route r fo type v vessel as equation (20).

$$\lambda_{r,v,f,t} = \frac{sm * SFC_f^{Base} * \left(0.455 * \left(\frac{s_{r,t}}{s_v^{Design}}\right)^6 - 0.71 * \left(\frac{s_{r,t}}{s_v^{Design}}\right)^3 + 1.28\right) * P_v^{me}}{{s_v^{Design}}^3} \qquad \forall r \in \mathcal{R}, \forall v \in \mathcal{V}_r, \forall f \in \mathcal{F}_v, \forall t \in \mathcal{T} \tag{19}$$

$$fc_{r,i,v,f,t}^{me} = \lambda_{r,v,f,t} {s_{r,t}}^3 t_{r,i,t}^{sea} \qquad \forall r \in \mathcal{R}, \forall i \in \mathcal{I}_r, \forall v \in \mathcal{V}_r, \forall f \in \mathcal{F}_v, \forall t \in \mathcal{T} \tag{20}$$

Auxiliary engine consumption is modelled linearly by time, using hourly consumption parameters $cp_{v,f}$ for different operational phases as Tran and Lam (2022) and Cariou et al. (2019): at sea, manoeuvring, and berthing (21). We calculate total fuel consumption and cost $C_{r,v,f,t}^{fc}$ (22) using engine fuel-specific price $p_{f,t}^{Fme}$ and $p_{f,t}^{Foe}$ for main engine fuel and other engines fuel, engine fuel-specific emission factor ε_f^{me} and ε_f^{oe}, carbon price p_t^C, and ETS zone parameter $x_{r,i}^{ets}$ (23).

$$fc_{r,i,v,f,t}^{oe} = t_{r,i,t}^{sea} cp_{v,f}^{sea} + t_{r,i,t}^{man} cp_{v,f}^{man} + t_{r,i,t}^{ber} cp_{v,f}^{ber} \qquad \forall r \in \mathcal{R}, \forall i \in \mathcal{I}_r, \forall v \in \mathcal{V}_r, \forall f \in \mathcal{F}_v, \forall t \in \mathcal{T} \tag{21}$$

$$C_{r,v,f,t}^{fc} = \sum_{i \in \mathcal{I}_r} \left[fc_{r,i,v,f,t}^{me} \left(p_{f,t}^{Fme} + x_{r,i}^{ets} \varepsilon_f^{me} p_t^C\right) + fc_{r,i,v,f,t}^{oe} \left(p_{f,t}^{Foe} + x_{r,i}^{ets} \varepsilon_f^{oe} p_t^C\right)\right] \qquad \forall r \in \mathcal{R}, \forall v \in \mathcal{V}_r, \forall f \in \mathcal{F}_v, \forall t \in \mathcal{T} \tag{22}$$

$$x_{r,i}^{ets} = \begin{cases} 1 & \text{if in ETS} \\ 0.5 & \text{if between non-ETS and ETS} \\ 0 & \text{if not in ETS} \end{cases} \qquad \forall r \in \mathcal{R}, \forall i \in \mathcal{I}_r \tag{23}$$

3.5 Carbon abatement measures

Two carbon abatement strategies are considered: energy-saving measures and fuel changes. Energy-saving measures reduce fuel consumption (Faber et al., 2011; Irena et al., 2021) and are quantified by a reduction rate $\tau^M_{v,m}$ for measure m within the set $\mathcal{M}$ and vessel type specific subset $\mathcal{M}_v$. The variable $m^M_{r,v,f,m,t}$ denotes the number of vessels implementing a measure. Measures may be mutually exclusive within subsets $\Theta_n \subset \mathcal{M}$ (24, 25) (Kesicki and Ekins, 2012; Irena et al., 2021).

$$\forall n \neq m, \Theta_n, \Theta_m \subseteq \mathcal{M}, \Theta_n \cap \Theta_m = \emptyset \tag{24}$$

$$\sum_{m \in \Theta_n} m^M_{r,v,f,m,t} \leq m^F_{r,v,f,t} \qquad \Theta_n \subset \mathcal{M}, \forall r \in \mathcal{R}, \forall v \in \mathcal{V}_r, \forall f \in \mathcal{F}_v, \forall n \in \mathcal{N}, \forall t \in \mathcal{T} \tag{25}$$

The variable $m^F_{r,v,f,t}$ represents the fuel type used by vessels, where f denotes the specific fuel being utilised at time t by vessel type v on route r, as described in equation (26). The set of available fuels $\mathcal{F}$ and subset $\mathcal{F}_v$ specify fuel options for each vessel type.

$$\sum_{f \in \mathcal{F}} m^F_{r,v,f,t} = m_{r,v,t} \qquad \forall r \in \mathcal{R}, \forall v \in \mathcal{V}_r, \forall t \in \mathcal{T} \tag{26}$$

Let now consider t^F_f and t^M_m as $t^F_f, t^M_m \in \mathcal{T}$ the years at with a technology m or a fuel f become available. We have (27) and (28) for fuel and measures respectively.

$$m^F_{r,v,f,t} = \begin{cases} 0 & t^F_f < t \\ m^F_{r,v,f,t} \geq 0 & t^F_f \geq t \end{cases} \qquad \forall t, t^F_f \in \mathcal{T}, \forall r \in \mathcal{R}, \forall v \in \mathcal{V}_r, \forall f \in \mathcal{F}_v \tag{27}$$

$$m^M_{r,v,f,m,t} = \begin{cases} 0 & t^M_m < t \\ m^M_{r,v,f,m,t} \geq 0 & t^M_m \geq t \end{cases} \qquad \forall t, t^M_m \in \mathcal{T}, \forall r \in \mathcal{R}, \forall v \in \mathcal{V}_r, \forall f \in \mathcal{F}_v, \forall m \in \mathcal{M}_v \tag{28}$$

3.6 Vessels age

We introduce $l \in \mathcal{L}_v$, the set of vessel ages, defined as $\mathcal{L}_v = \{1, \ldots, n^V_v + 1\}$, where n^V_v is the life expectancy of a vessel of type v. We define new variables for the vessels as follows: $m^V_{v,t}$ represents the number of deployed vessels of type v in the fleet at year t as (29), and $m^L_{v,l,t}$ represents the number of vessels of type v and age l at year t. Consequently, the temporal dynamics of these variables are governed by the life expectancy n^V_v of vessels of type v, leading to equation (30) and (31).

$$m^V_{v,t} = \text{‘}\sum_{r \in \mathcal{R}} m_{r,v,t} \qquad \forall v \in \mathcal{V}, \forall t \in \mathcal{T} \tag{29}$$

$$m^V_{v,t} = \sum_{\substack{l \in \mathcal{L}_v \\ l \leq n^V_v}} m^L_{v,l,t} \qquad \forall v \in \mathcal{V}, \forall t \in \mathcal{T} \tag{30}$$

$$m^L_{v,l+1,t+1} = m^L_{v,l,t} \qquad \forall v \in \mathcal{V}, \forall l \in \mathcal{L}_v, \forall t \in \mathcal{T} \tag{31}$$

We do the same with fuel-vessels variable $m^{FL}_{v,f,l,t}$ (32, 33), and measures vessels variables $m^{ML}_{v,f,m,l,t}$ considering that during vessels life cycle, we can retrofit using energy-saving measures (34, 35). We have $m^L_{v,l+1,t+1}, m^{FL}_{v,f,l,t}, m^{ML}_{v,f,m,l,t} \in \mathbb{N}$.

$$\sum_{\substack{l \in \mathcal{L}_v \\ l \leq n^F_f}} m^{FL}_{v,f,l,t} = \sum_{r \in \mathcal{R}} m^F_{r,v,f,t} \qquad \forall v \in \mathcal{V}, \forall f \in \mathcal{F}_v, \forall t \in \mathcal{T} \tag{32}$$

$$m^{FL}_{v,f,l+1,t+1} = m^{FL}_{v,f,l,t} \qquad \forall v \in \mathcal{V}, \forall f \in \mathcal{F}_v, \forall l \in \mathcal{L}_v, \forall t \in \mathcal{T} \tag{33}$$

$$\sum_{\substack{l\in\mathcal{L}_v\\ l\le n^M_m}} m^{ML}_{v,f,m,l,t} = \sum_{r\in\mathcal{R}} m^{M}_{r,v,f,m,t} \qquad \forall v\in\mathcal{V}, \forall f\in\mathcal{F}_v, \forall m\in\mathcal{M}_v, \forall t\in\mathcal{T} \tag{34}$$

$$m^{ML}_{v,f,m,l+1,t+1} \ge m^{ML}_{v,f,m,l,t} \qquad \forall v\in\mathcal{V}, \forall f\in\mathcal{F}_v, \forall m\in\mathcal{M}_v, \forall l\in\mathcal{L}_v, \forall t\in\mathcal{T} \tag{35}$$

3.7 Capital

We introduce vessel-type capital stock with K^V_v as (36) using capital depreciation rate δ^K. Then we consider the cost of vessel capital $C^{K^V}_t$ with (37) following the same method as static model. Similarly, we consider the capital dynamics for fuels $K^F_{v,f}$ and measures $K^M_{v,f,m}$ with (38, 39) and (40, 41) respectively.

$$K^V_{v,t} = \sum_{\substack{l\in\mathcal{L}_v\\ l\le n^V_v}} m^L_{v,l,t} p^V_v \left(1-\delta^K\right)^{l-1} v \qquad \forall v\in\mathcal{V}, \forall t\in\mathcal{T} \tag{36}$$

$$C^{K^V}_t = \sum_{v\in\mathcal{V}} K^V_{v,t} \frac{r^K}{1-(1+r^K)^{-n^V_v}} \qquad \forall t\in\mathcal{T} \tag{37}$$

$$K^F_{v,f,t} = \sum_{\substack{l\in\mathcal{L}_v\\ l\le n^F_f}} m^{FL}_{v,f,l,t} p^F_{v,f} \left(1-\delta^K\right)^{l-1} \qquad \forall v\in\mathcal{V}, \forall f\in\mathcal{F}_v, \forall t\in\mathcal{T} \tag{38}$$

$$C^{K^F}_t = \sum_{v\in\mathcal{V}} \sum_{f\in\mathcal{F}_v} K^F_{v,f,t} \frac{r^K}{1-(1+r^K)^{-n^F_f}} \qquad \forall t\in\mathcal{T} \tag{39}$$

$$K^M_{v,f,m,t} = \sum_{\substack{l\in\mathcal{L}_v\\ l\le n^M_m}} m^{ML}_{v,f,m,l,t} p^M_{v,m} \left(1-\delta^K\right)^{l-1} \qquad \forall v\in\mathcal{V}, \forall f\in\mathcal{F}_v, \forall m\in\mathcal{M}_v, \forall t\in\mathcal{T} \tag{40}$$

$$C^{K^M}_t = \sum_{v\in\mathcal{V}} \sum_{f\in\mathcal{F}_v} \sum_{m\in\mathcal{M}_v} K^M_{v,f,m,t} \frac{r^K}{1-(1+r^K)^{-n^M_m}} \qquad \forall t\in\mathcal{T} \tag{41}$$

3.8 Costs

The firm's total annual voyage cost (42) includes fuel and carbon costs, plus an exogenous port entrance fee c^{entr}_v and canal fee $c^{canal2}_{r,v}$, multiplied by the number of annual round-trips. We subtract from fuel consumption the energy savings made possible by measures, using a geometric average weighted by the share of vessels applying this measure on vessels of type v using fuel f on route r ($\prod_{m\in\mathcal{M}_v} \left(1-\tau^M_{v,m}\right)^{x^M_{r,v,f,om,t}}$). For this we set $x^M_{r,v,f,om,t}$ as the ratio between vessels using fuel f applying measure m and vessels using fuel f, and we write it as (43) to avoid undefined fraction error.

Operating costs encompass expenses for spare parts, lubricants, auxiliary fuel, maintenance, repair, crew, and administration (Herrera Rodriguez et al., 2022), represented by c^{opr}_v (44).

$$C^V_t = \sum_{r\in\mathcal{R}} \sum_{v\in\mathcal{V}_r} \left(\sum_{f\in\mathcal{F}_v} \left[\left(\prod_{m\in\mathcal{M}_v} \left(1-\tau^M_{v,m}\right)^{x^M_{r,v,f,m,t}} \right) m^F_{r,v,f,t} C^{fc}_{r,v,f,t} \right] + m_{r,v,t}(c^{canal}_{r,v} + N_r c^{entr}_v) \right) \Phi_{r,t} \qquad \forall t\in\mathcal{T} \tag{42}$$

[2] Which includes the number of transits through the canal on a round trip.

$$x^M_{r,v,f,m,t} m^F_{r,v,f,t} = m^M_{r,v,f,m,t} \qquad \forall r \in \mathcal{R}; \forall v \in \mathcal{V}_r; \forall f \in \mathcal{F}_v; \forall m \in \mathcal{M}_v, \forall t \in \mathcal{T} \tag{43}$$

$$C^O_t = \sum_{r \in \mathcal{R}} \sum_{v \in \mathcal{V}_r} m_{r,v,t} c^{opr}_v \qquad \forall t \in \mathcal{T} \tag{44}$$

We includes cargo-handling cost C^{CH}_t using time spent berthing and vessel-type specific hourly cost c^{ber}_v (45).

$$C^{CH}_t = \sum_{r \in \mathcal{R}} \sum_{v \in \mathcal{V}_r} \sum_{i \in \mathcal{I}_r} m_{r,v,t} t^{ber}_{r,i,t} c^{ber}_v \phi_{r,t} \qquad \forall t \in \mathcal{T} \tag{45}$$

Some measures incur recurring annual costs, denoted by $c^M_{v,m}$ (46).

$$C^M_t = \sum_{r \in \mathcal{R}} \sum_{v \in \mathcal{V}_r} \sum_{f \in \mathcal{F}_v} \sum_{m \in \mathcal{M}_v} m^M_{r,v,f,m,t} c^M_{v,m} \qquad \forall t \in \mathcal{T} \tag{46}$$

We set C^K_t total annual capital cost as equation (47).

$$C^K_t = C^{K^V}_t + C^{K^F}_t + C^{K^M}_t \qquad \forall t \in \mathcal{T} \tag{47}$$

3.9 Objective function

As classic time dynamic model, we introduce discount rate ρ intro the objective function with (48).

$$\sum_{t \in \mathcal{T}} (1+\rho)^{-t} \left(C^V_t + C^O_t + C^{CH}_t + C^M_t + C^K_t \right) \tag{48}$$

The full program (51) tends to minimise total discounted cost on t^{max} periods to obtain decision vectors $\mathcal{X}^{T^*}_1$ (49) and $\mathcal{X}^{T^*}_2$ (50).

$$\mathcal{X}^{T^*}_1 = \left\{ {s_{r,t}}^*, {m_{r,v,t}}^*, {m^M_{r,v,f,m,t}}^*, {m^F_{r,v,f,t}}^* | r \in \mathcal{R}; v \in \mathcal{V}_r; m \in \mathcal{M}_v; f \in \mathcal{F}_v : t \in \mathcal{T} \right\} \tag{49}$$

$$\mathcal{X}^{T^*}_2 = \{ {lo_{o,r,v,i,t}}^*, {di_{o,r,v,i,t}}^*, {fl_{o,r,v,i,t}}^* | o \in \mathcal{P}; r \in \mathcal{R}; v \in \mathcal{V}_r; i \in \mathcal{I}_r; t \in \mathcal{T} \} \tag{50}$$

$$
\begin{aligned}
\min_{\mathcal{X}_1^*,\mathcal{X}_2^*} \quad & \sum_{t\in\mathcal{T}} (1+\rho)^{-t} \left(C_t^V + C_t^O + C_t^{CH} + C_t^M + C_t^{K^V} + C_t^{K^M} + C_t^{K^F} \right) \\
\text{s.t.} \quad & C_t^V = \sum_{r\in\mathcal{R}} \sum_{v\in\mathcal{V}_r} \left(\sum_{f\in\mathcal{F}_v} \left[\left(\prod_{m\in\mathcal{M}_v} \left(1-\tau_{v,m}^M\right)^{x_{r,v,f,m,t}^M} \right) m_{r,v,f,t}^F C_{r,v,f,t}^{fc} \right] + m_{r,v,t} N_r c_v^{entr} \right) \Phi_{r,t} \\
& C_t^O = \sum_{r\in\mathcal{R}} \sum_{v\in\mathcal{V}_r} m_{r,v,t} c_v^{opr} \\
& C_t^{CH} = \sum_{r\in\mathcal{R}} \sum_{v\in\mathcal{V}_r} \sum_{i\in\mathcal{I}_r} m_{r,v,t} t_{r,i,t}^{ber} c_v^{ber} \phi_{r,t} \\
& C_t^M = \sum_{r\in\mathcal{R}} \sum_{v\in\mathcal{V}_r} \sum_{f\in\mathcal{F}_v} \sum_{m\in\mathcal{M}_v} m_{r,v,f,m,t}^M c_{v,m}^M \\
& C_t^{K^V} = \sum_{v\in\mathcal{V}} \sum_{\substack{l\in\mathcal{L}_v \\ l\le n_v^V}} m_{v,l,t}^L p_v^V \left(1-\delta^K\right)^{l-1} \frac{r^K}{1-(1+r^K)^{-n_v^V}} \\
& C_t^{K^F} = \sum_{v\in\mathcal{V}} \sum_{f\in\mathcal{F}_v} \sum_{\substack{l\in\mathcal{L}_v \\ l\le n_f^F}} m_{v,f,l,t}^{FL} p_{v,f}^F \left(1-\delta^K\right)^{l-1} \frac{r^K}{1-(1+r^K)^{-n_f^F}} \\
& C_t^{K^M} = \sum_{v\in\mathcal{V}} \sum_{f\in\mathcal{F}_v} \sum_{m\in\mathcal{M}_v} \sum_{\substack{l\in\mathcal{L}_v \\ l\le n_m^M}} m_{v,f,m,l,t}^{ML} p_{v,m}^M \left(1-\delta^K\right)^{l-1} \frac{r^K}{1-(1+r^K)^{-n_m^M}} \\
& C_{r,v,f,t}^{fc} = \sum_{i\in\mathcal{I}_r} \left[\lambda_{r,v,f,t} {s_{r,t}}^3 t_{r,i,t}^{sea} \left(p_{f,t}^{Fme} + x_{r,i}^{ets} \varepsilon_f^{me} p_t^C \right) + \left(t_{r,i,t}^{sea} cp_{v,f}^{sea} + t_{r,i,t}^{man} cp_{v,f}^{man} + t_{r,i,t}^{ber} cp_{v,f}^{ber} \right) \left(p_{f,t}^{Foe} + x_{r,i}^{ets} \varepsilon_f^{oe} p_t^C \right) \right] && \forall r \in \mathcal{R}, \forall v \in \\
& \lambda_{r,v,f,t} = \frac{sm * SFC_f^{Base} * \left(0.455 * \left(\frac{s_{r,t}}{s_v^{Design}} \right)^6 - 0.71 * \left(\frac{s_{r,t}}{s_v^{Design}} \right)^3 + 1.28 \right) * P_v^{me}}{{s_v^{Design}}^3} && \forall r \in \mathcal{R}, \forall v \in \\
& t_{r,i,t}^{tot} = \frac{d_{r,i}}{s_{r,t}} + t_{r,i,t}^{man} + \max_v \left(\sum_{o\in\mathcal{P}} \left[lo_{o,r,v,i,t} + di_{o,r,v,i,t} \right] tp_v^{ber} \right) && \forall r \\
& \phi_{r,t} = \frac{365*24}{\sum_{i\in\mathcal{I}_r} t_{r,i,t}^{tot}} \\
& m_{v,t}^V = \text{`} \sum_{r\in\mathcal{R}} m_{r,v,t} \\
& m_{v,t}^V = \sum_{\substack{l\in\mathcal{L}_v \\ l\le n_v^V}} m_{v,l,t}^L \\
& m_{v,l+1,t+1}^L = m_{v,l,t}^L && \forall v \\
& \sum_{\substack{l\in\mathcal{L}_v \\ l\le n_f^F}} m_{v,f,l,t}^{FL} = \sum_{r\in\mathcal{R}} m_{r,v,f,t}^F && \forall v \\
& m_{v,f,l+1,t+1}^{FL} = m_{v,f,l,t}^{FL} && \forall v \in \mathcal{V}, \forall f \\
& \sum_{\substack{l\in\mathcal{L}_v \\ l\le n_m^M}} m_{v,f,m,l,t}^{ML} = \sum_{r\in\mathcal{R}} m_{r,v,f,m,t}^M && \forall v \in \mathcal{V}, \forall f \in \\
& m_{v,f,m,l+1,t+1}^{ML} \ge m_{v,f,m,l,t}^{ML} && \forall v \in \mathcal{V}, \forall f \in \mathcal{F}_v, \forall m \in \\
& \sum_{v\in\mathcal{V}} \left(fl_{o,r,v,i-1,t} + lo_{o,r,v,i,t} - di_{o,r,v,i,t} \right) = \sum_{v\in\mathcal{V}} fl_{o,r,v,i,t} && \forall o \in \mathcal{P}, \forall r \\
& \sum_{v\in\mathcal{V}} \left(fl_{o,r,v,N_r,t} + lo_{o,r,v,0,t} - di_{o,r,v,0,t} \right) = \sum_{v\in\mathcal{V}} fl_{o,r,v,0,t} && \forall \\
& \sum_{o\in\mathcal{P}} fl_{o,r,v,i,t} \le cap_v && \forall r \in \mathcal{R}, \forall v \\
& \sum_{r\in\mathcal{R}} \sum_{\substack{i\in\mathcal{I}_r \\ p_{r,i}=d}} \phi_{r,t} m_{r,v,t} (lo_{o,r,v,i,t} - di_{o,r,v,i,t}) = df_{o,d,v,t} && d \ne o, \forall (o, d \\
& \sum_{v\in\mathcal{V}} df_{o,d,v,t} = D_{o,d,t} \\
& lo_{p,v,t} = \sum_{d\in\mathcal{P}} df_{p,d,v,t} && \forall \\
& di_{p,v,t} = \sum_{o\in\mathcal{P}} df_{o,p,v,t} && \forall \\
& tr_{p,v,t} = \sum_{r\in\mathcal{R}} \sum_{\substack{i\in\mathcal{I}_r \\ p_{r,i}=p}} \sum_{o\in\mathcal{P}} lo_{o,r,v,i,t} - lo_{p,v,t} && \forall \\
& \sum_{m\in\Theta_n} m_{r,v,f,m,t}^M \le m_{r,v,f,t}^F && \Theta_n \subset \mathcal{M}, \forall r \in \mathcal{R}, \forall v \in \mathcal{V}_r, \forall f \\
& \sum_{f\in\mathcal{F}} m_{r,v,f,t}^F = m_{r,v,t} && \forall r \\
& x_{r,v,f,m,t}^M m_{r,v,f,t}^F = m_{r,v,f,m,t}^M \forall r \in \mathcal{R}; \forall v \in \mathcal{V}_r; \forall f \in \mathcal{F}_v; \forall m \in \mathcal{M}_v, \forall t \in \mathcal{T}
\end{aligned}
\tag{51}
$$

4 Application

4.1 General data

By means of the software GAMS using Mixed Integer Non Linear Solver SBB (Standard Branch and Bound), we minimise the total annual cost of the representative shipping company, operating on six routes (cma-cgm.fr), at given pair-port demands. We estimated distances between ports for the six following routes (searoutes.com, Appendix A): French Asia Line 1 (FAL1), French Asia Line 3 (FAL3), Europe Pakistan India Consortium (EPIC), Bosphorus Express (BEX), Phoenician Express (BEX2), and Mediterranean Club Express (MEX). It is assumed that only one type of vessel is accepted per route because of the homogeneity in size of the vessels operated by CMA CGM on the chosen routes as $Card(\mathcal{V}_r) = 1, \forall r \in \mathcal{R}$. We consider that CMA CGM's choice is informed and justified by characteristics associated with the transit ports and the route (see Table 1).

Route	**Duration** *in days*	**Vessels** *number*	**Port** *calls*	**Vessels** *type*
r	$T0_r^{tot}$	m_v^0	N_r	$v \in \mathcal{V}_r$
FAL1	98	12	12	Large
FAL3	84	10	11	Large
EPIC	63	6	15	Medium
BEX	70	5	14	Small
BEX2	70	3	12	Small
MEX	91	9	17	Large

Table 1: Route characteristics

The base fleet made of 45 vessels is disaggregated into three capacity types: small vessels (8000 TEU), medium (12000 TEU) and large vessels (18000 TEU). We document the operational cost, port entrance fee, berthing time and cost from Herrera Rodriguez et al. (2022) converted to 2024US$. For new ships costs, we use three vessel type costs (small: \$100M, medium: \$120M, large: \$150M) in line with Murray (2016); IHS (2015).

Vessel type	**Capacity** *TEU*	**Operating cost** *\$M/year*	**Port-entrance fee** *\$/port calls*	**Bething time** *hour/TEU*	**Berthing cost** *\$/hour*	**Price** *\$M*
v	cap_v	c_v^{opr}	c_v^{entr}	tp_v^{ber}	c_v^{ber}	p_v^V
Small	8000	4.79	10,373	0.008	2518.95	100
Medium	12000	6.29	13,831	0.007	4678.05	120
Large	18000	7.79	18,442	0.006	5877.55	150

Table 2: Cost data by vessel type

Engine Type	Fuel Type	SFC	SFC*(MDO)*	SFC*(Total)*
		g/kWh	g/kWh	g/kWh
	f			SFC_f^{Base}
Slow-speed diesel	HFO	175.0	-	175.0
	VLSFO	175.1	-	175.1
	MDO	165.0	-	165.0
	MeOH	350.0	-	350.0
LNG-Otto (Slow-speed)	LNG-Otto	148.0	0.8	148.8
LNG-Diesel (Slow-speed)	LNG-Diesel	135.0	6	141.0
LBSI	LBSI	156.0	-	156.0
Hydrogen ICE	H2-ICE	58.7	-	58.7

Table 3: Specific fuel consumption in g/kWh by engine type and fuel type for main engine

4.2 Fuel consumption

4.2.1 Main engine

We consider six types of fuel with Very Low Sulfur Fuel Oil (VLSFO) as base fuel[3], Methanol (MeOH), Dual Fuel Liquified Natural Gas - Diesel with Otto mothod [4] (LNG-Otto), Dual Fuel Liquified Natural Gas - Diesel [5] (LNG-Diesel) and Liquified Natural Gas Lean Burn Spark-Ignited[6] (LBSI) and Hydrogen Internal Combustion Engine (H2-ICE). MAN Energy Solutions (2024) provides the main engine power for vessels with capacities of 8000 TEU, 12000 TEU, and 18000 TEU, which are 52,566 kW, 57,901 kW, and 60,202 kW, respectively. The average design speed for all three capacities is 22 knots. Data concerning SFC come from Faber et al. (2021) for Heavy fuel oil (HFO), MeOH, LNG-Otto, LNG-Diesel and LBSI. As Very Low Sulfur Oil is one of the principal fuel currently[7], and is part of heavy fuel oil, we computed its SFC parameter. VLSFO is less energy dense than classic HFO, thus, we computed the ratio of both gravimetric energy density $ed_f(MJ/m^3)/d_f(kg/m^3)$ and multiplied it by the HFO base SFC (52). We do not have data for Hydrogen consumption so we compute its SFC in the same way as VLSFO using gravimetric energy density from Møller et al. (2017) (120 MJ/kg). For dual fuels, for dual fuel options, we add up the SFCs of the two types of fuel. As Cariou et al. (2019), we set the sea margin at 10%. All the data obtained are shown in table 3. Figure 1 shows hourly fuel consumption for large vessels using VLSFO.

$$SFC_{vlsfo} = SFC_{hfo}\frac{ed_{hfo}/d_{hfo}}{ed_{vlsfo}/d_{vlsfo}} \tag{52}$$

$$SFC_{vlsfo} = 175 * \frac{39,396/980}{37,766/940} \tag{53}$$

$$SFC_{vlsfo} = 175.1 \tag{54}$$

[3]Which is the common fuel after the tightening of the policy on sulphur emissions.

[4]A dual-fuel engine that uses pre-mixed LNG and air, ignited by a spark or small diesel pilot, operating at low pressure.

[5]A dual-fuel engine that injects LNG at high pressure, using compression ignition with a small amount of diesel.

[6]A spark-ignited engine that runs on LNG with a lean air-fuel mixture.

[7]After he tightening of IMO policy on sulfur oxides emissions.

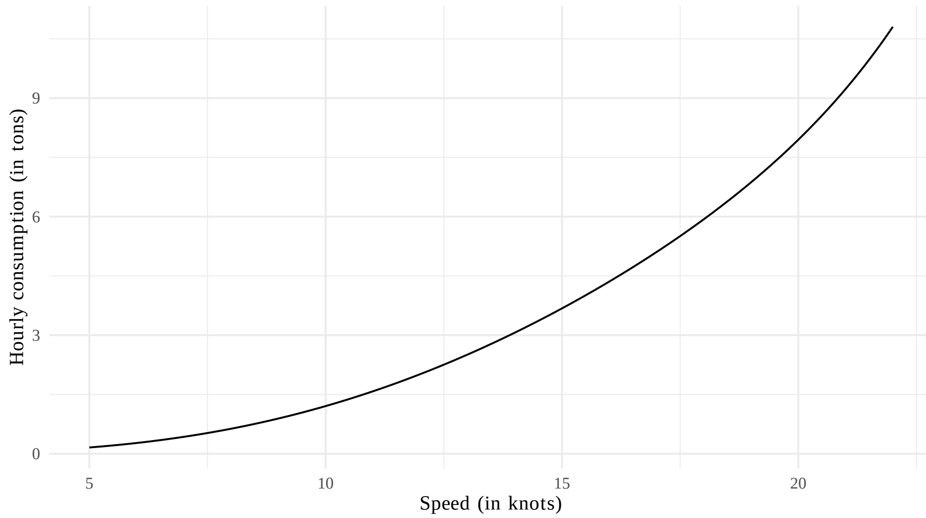

Figure 1: Hourly fuel consumption in tons according to speed in knots for a large containership (18000 TEU) using VLSFO

4.2.2 Auxiliary engines and boiler

Let e be the index of engine such as $e \in \{aux, boi\}$ and a be the index of vessel activity such as $a \in \{ber, man, sea\}$. According to Faber et al. (2021), auxiliary engine and boiler engine fuel consumption per hour can be computed as the multiplication of base SFC and power output of vessels with (55). We used both power output (see table 5) and SFC for our three type of vessels from Faber et al. (2021). For VLSFO, Methanol and Hydrogen, we do not have SFC so we do as (52) using gravimetric energy density. For dual-fuel engines, we keep the main fuel for the auxiliary engines and boiler. SFC data are shown in table 4. We used 5000-8000 TEU data for aux/boil engine power of 8000 TEU, 8000-12000 TEU for 12000 TEU and 14500-20000 TEU for 18000 TEU.

$$fc_{v,e,a,f} = kW^{output}_{v,e,a} SFC^{oe}_{e,f} \qquad \forall v \in \mathcal{V}; \forall e \in \{aux, boi\}; \forall a \in \{ber, man, sea\}; \forall f \in \mathcal{F}_v \tag{55}$$

Our estimation results are shown in table 6. From these results we computed $cp^a_{v,f}$ which is the sum of both engines for each activity as (56). $cp^a_{v,f}$ values are shown in table 7.

$$cp^a_{v,f} = \sum_{e \in \{aux, boi\}} fc_{v,e,a,f} \qquad \forall v \in \mathcal{V}; \forall f \in \mathcal{F}_v; \forall a \in ber, man, sea \tag{56}$$

4.3 Carbon emission factor and fuel price

For each engine and fuel we consider carbon emission factor ε^{me}_f and ε^{oe}_f from Comer and Osipova (2021) and MAN Energy Solutions (2024) using "CO2 tank-to-wake" data: 3.206 g^{CO_2}/g^{fuel} for MDO, 3.114 g^{CO_2}/g^{fuel} for HFO and VLSFO, 2.750 g^{CO_2}/g^{fuel} for LNG, 1.375 g^{CO_2}/g^{fuel} for MeOH and 0 g^{CO_2}/g^{fuel} for Hydrogen. For dual fuel engines, we compute emission factor using fuel specific SFC share in total SFC using (57) with $f1$ and $f2$ main fuel and secondary fuel respectively. We consider that other engines consume only the main fuel so that $\varepsilon^{oe}_f = \varepsilon_{f1}$. We do the same with fuel prices $p^{Fme}_{f,t}$ and $p^{Foe}_{f,t}$. Data about emission factor and fuel price are summarised in table 8.

$$\varepsilon^{me}_f = \frac{SFC_{f1}}{SFC^{Total}_f} \varepsilon_{f1} + \frac{SFC_{f2}}{SFC^{Total}_f} \varepsilon_{f2} \tag{57}$$

Engine Type	**Fuel Type**	**SFC**
		g/kWh
e	f	$SFC^o e_e, f$
Auxiliary engines	VLSFO	195.1
	LNG (All)	156.0
	MeOH	394.0
	H2-ICE	65.3
Steam turbines (and boilers)	VLSFO	340.2
	LNG (All)	285.0
	MeOH	686.9
	H2-ICE	113.9

Table 4: Specific fuel consumption in g/kWh by engine type and fuel type for other engines

Engine Type	**Activity**	**Power output**		
			kWh	
e	a	$kW^{output}_{small,e,a}$	$kW^{output}_{medium,e,a}$	$kW^{output}_{large,e,a}$
Auxiliary	Berth	590	620	630
	Manoeuvring	550	540	630
	At sea	0	0	0
Boiler	Berth	1100	1150	1400
	Manoeuvring	2800	2900	3600
	At sea	1450	1800	2300

Table 5: Power output by vessel type and activity for auxiliary and boiler engines in kW

Engine Type	**Fuel Type**	**Activity**	**Consumption parameter**		
				mt/h	
e	f	a	fc_small, e, a, f	fc_medium, e, a, f	fc_large, e, a, f
Boiler	VLSFO	Berth	0.374	0.391	0.476
		Manoeuvring	0.953	0.987	1.225
		At Sea	0.493	0.612	0.782
	LNG (All)	Berth	0.314	0.328	0.399
		Manoeuvring	0.798	0.827	1.026
		At Sea	0.413	0.513	0.656
	MeOH	Berth	0.756	0.790	0.962
		Manoeuvring	1.923	1.992	2.473
		At Sea	0.996	1.236	1.580
	H2	Berth	0.125	0.131	0.159
		Manoeuvring	0.319	0.330	0.410
		At Sea	0.165	0.205	0.262
Auxiliary	VLSFO	Berth	0.115	0.121	0.123
		Manoeuvring	0.107	0.105	0.123
		At Sea	-	-	-
	LNG (All)	Berth	0.092	0.097	0.098
		Manoeuvring	0.086	0.084	0.098
		At Sea	-	-	-
	MeOH	Berth	0.232	0.244	0.248
		Manoeuvring	0.217	0.213	0.248
		At Sea	-	-	-
	H2	Berth	0.039	0.041	0.041
		Manoeuvring	0.036	0.035	0.041
		At Sea	-	-	-

Table 6: Hourly fuel consumption in tons for auxiliary engines and boilers by fuel type and activity for small, medium, and large vessels

Fuel Type	**Activity**	**Consumption parameter** mt/h		
f	a	$cp^{a}_{s}mall, f$	$cp^{a}_{m}edium, f$	$cp^{a}_{l}arge, f$
	Berth	0.489	0.512	0.599
VLSFO	Manoeuvring	1.060	1.092	1.348
	At Sea	0.493	0.612	0.782
	Berth	0.406	0.424	0.497
LNG (All)	Manoeuvring	0.884	0.911	1.124
	At Sea	0.413	0.513	0.656
	Berth	0.988	1.034	1.210
MeOH	Manoeuvring	2.140	2.205	2.721
	At Sea	0.996	1.236	1.580
	Berth	0.164	0.171	0.201
H2	Manoeuvring	0.355	0.366	0.451
	At Sea	0.165	0.205	0.262

Table 7: Cumulative hourly fuel consumption for auxiliary engines and boiler in tons by activity and vessel type

Fuel Type	**ME emission factor**	**OE emission factor**	**ME fuel price**	**OE fuel price**
	g^{CO_2}/g^{fuel}	g^{CO_2}/g^{fuel}	$\$2024/mt$	$\$2024/mt$
f	ε_f^{me}	ε_f^{oe}	p_f^{Fme}	p_f^{Foe}
VLSFO	3.114	3.114	554.0	554.0
MeOH	4.375	4.375	340.0	340.0
LNG-Otto	2.752	2.750	668.5	668.0
LNG-Diesel	2.769	2.750	671.7	668.0
LBSI	2.750	2.750	668.0	668.0
H2-ICE	0.000	0.000	4000.0	4000.0

Table 8: Emission factor and fuel price by fuel type and engine type

4.4 Energy-saving measures and fuel investment cost

For Energy-saving measures, we consider technical measures Faber et al. (2021). “Some Mitigation Measures might be correlated meaning that they can reduce emissions in the same way or cannot be applied simultaneously due to physical constraints” (Kesicki and Ekins, 2012; Irena et al., 2021), in this way we define 12 subsets $\Theta_n \subset \mathcal{M}$ grouping measures that are not applicable at the same time, these subsets are shown in Appendix table 12. Each measure is rated on a maturity scale from 1 to 4. A rating of 1 means the technology is available now or within 5 years, while 2 indicates availability after 5 years. Levels 3 and 4 represent evolving technologies, with expected availability we set at 10 and 20 years, respectively. The data of non-recurring cost, recurring costs and abatement potential for each measure are aggregated from several sources, all the work is shown in Appendix B.

For alternative fuels investment cost, we estimated value using investment data from Brynolf (2014); Grahn et al. (2013).As annualised capital cost needs life expectancy data, life expectancy for all vessels and fuel change investment is set to 25 years following Dinu and Ilie (2015) with $n_v^V = n_f^F = 25$. The life cycle of each measure depends strongly on the type of measure chosen. We use life cycle data from Faber et al. (2011) summarised in appendix table 12.

4.5 Demand

We lack specific demand data for each port pair. To address this, we use the round-trip duration provided by CMA CGM, base fleet data, assuming an average speed of 16 knots for each route. By maximizing total demand, we derive an approximate demand per port pair that aligns with the typical operation of the vessels.

5 Preliminary results

This section presents preliminary simulation results from our fleet deployment model, aimed at understanding fleet management decisions and trade-offs with decarbonization strategies. Due to the model's computational complexity and long calculation times, we limited the analysis to a single year, providing a snapshot of the fleet's response to various conditions. Capital expenses for ships and decarbonization technologies are treated as first-year costs, based on a formula that considers vessel age. Despite focusing on a single year, this approach still offers meaningful insights into the financial and operational impacts of decarbonization strategies.

We simulate two scenarios: one without energy-saving measures or alternative fuels, and another where both are introduced to simulate a decarbonization-focused environment. These scenarios examine how carbon pricing affects vessel behaviour and emissions under different technological constraints. The model applies a carbon price to all fleet emissions, with values ranging from \$0 to \$400 per tonne of CO2 equivalent.

The following sections will detail the results, highlighting interactions between fleet deployment, costs, vessel speed, and emissions under various carbon pricing schemes.

5.1 Speed management

As expected, an increase in carbon pricing leads to a reduction in vessel speed, with a progressive and differentiated decline across routes in both scenarios (see figure 2-3).

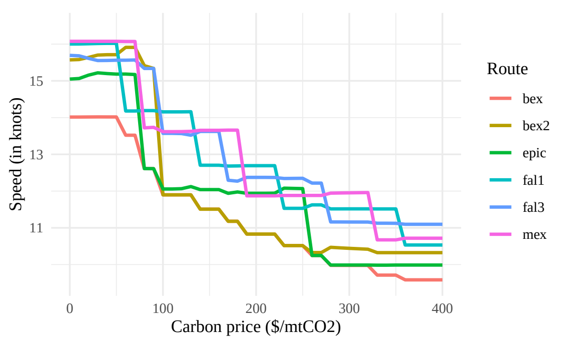

Figure 2: Speed in knots per route without energy-saving, under a carbon tax of 0–400\$/mtCO2

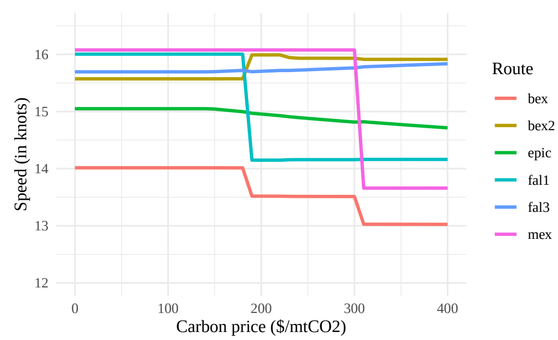

Figure 3: Speed in knots per route with energy-saving, under a carbon tax of 0–400\$/mtCO2

Without energy-saving measures, vessel speeds drop more sharply in response to carbon pricing. For instance, we observe a substantial decrease in speed around a carbon price of \$80 per tonne, whereas in the scenario with energy-saving measures, a similar drop does not occur until a carbon price around \$200 per tonne: when no technological solutions are available to reduce energy consumption, ship operators rely more heavily on reducing speed as a primary strategy to mitigate carbon costs.

The relationship between carbon price and average vessel speed is almost linear in both scenarios, but the rate of speed reduction differs (see figure 4). Without EM, the average speed decreases by -0.096% for each additional dollar of carbon price and with EM, this rate of decline is more moderate at -0.063% per dollar.

At the highest simulated carbon price of \$400 per tonne, the difference between the scenarios becomes more pronounced: the fleet's average speed drops by 32% without EM, while with these measures, the reduction is limited to 23%. This 9-percentage-point difference underscores how energy-saving technologies not only help operators reduce emissions but also maintain higher operational speeds, which can be crucial for maintaining shipping schedules and overall fleet efficiency

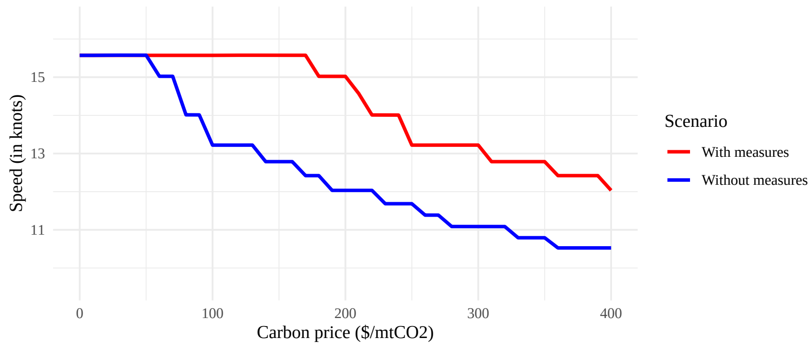

Figure 4: Average speed with and without measures, under a carbon tax of 0–400$/mtCO2

5.2 Fleet expansion

The number of vessels deployed on each route follows an inverse dynamic to vessel speed. This adjustment is a direct response to slower transit times, as more ships are needed to maintain cargo throughput and service reliability (see figure 5-6).

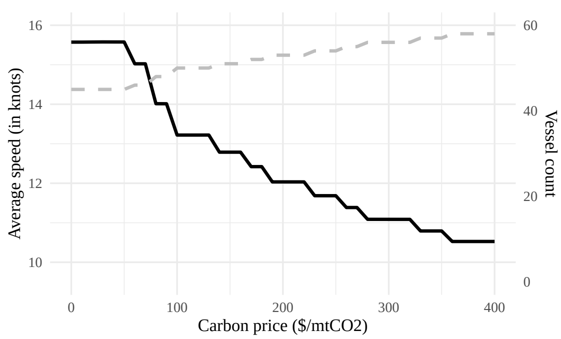

Figure 5: Total fleet size and average speed without energy-saving, under a carbon tax of 0–400$/mtCO2

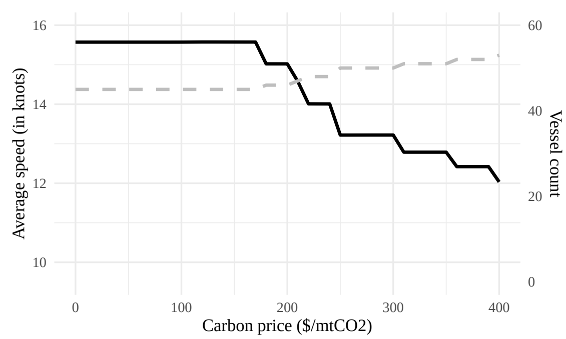

Figure 6: Total fleet size and average speed with energy-saving, under a carbon tax of 0–400$/mtCO2

In the absence of EM, the fleet sees a significant expansion, with fleet increase by around 30% at a carbon price of $400 per tonne. When EM are available, the increase in fleet size is less drastic. At a carbon price of $400 per tonne, the fleet size grows by 18%, a more moderate adjustment. The presence of energy-saving technologies allows operators to mitigate the need for fleet expansion.

Across both scenarios, the proportion of each vessel type in the fleet remains relatively constant (see figure 7-8). This stability is a result of the model's assumption that each route is served by a single vessel type and constant demand, meaning that although the number of vessels changes, the fleet composition by type does not.

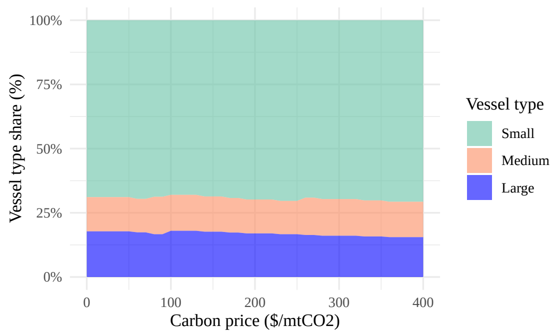

Figure 7: Fleet type share without energy-saving, under a carbon tax of 0–400$/mtCO2

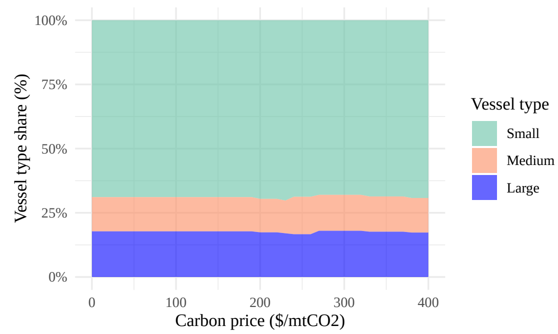

Figure 8: Fleet type share with energy-saving, under a carbon tax of 0–400$/mtCO2

5.3 Costs evolution

The total cost of maritime operations is significantly impacted by the introduction of carbon pricing. In the absence of EM, each additional dollar of carbon tax leads to an average increase of $2.4 million in total costs, translating to an average rise of 0.062%. At the upper end of the carbon price spectrum, when the price reaches $400 per tonne of carbon emissions, this results in a 28% increase in total costs compared to a baseline scenario without carbon pricing. In contrast, when energy-saving measures are available, the total cost increases at a slower rate. Each dollar of carbon tax results in an average total cost increase of $2.1 million, or 0.056%. At a carbon price of $400 per tonne, total costs rise by 19%, a notable reduction compared to the scenario without these measures. Figure 9 shows the cost evolution relative to no carbon price, no measures state.

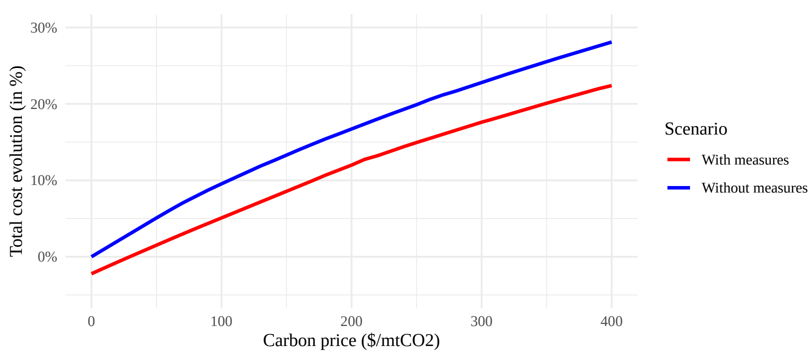

Figure 9: Total cost evolution (in %) for the 2 scenarios compared to no carbon price no measure state, under a carbon tax of 0–400$/mtCO2

In both scenarios, voyage costs experience only a modest increase as the price of carbon rises (see figure 10-11). This is largely due to the compensatory effect of reduced fuel consumption, which offsets the rising carbon-related costs. As vessel speeds decrease and energy-saving measures are implemented, fuel consumption declines, leading to lower overall fuel costs. Consequently, we observe an asymptotic trend in the carbon-related portion of voyage costs in both scenarios (see figure 12-13), indicating that the cost of the carbon price is partially absorbed by fuel consumption drop. Capital expenditures, however, show a much more pronounced increase, particularly when energy-saving measures are not available. The surge in capital costs is driven primarily by the significant increase in the number of vessels deployed to compensate for slower operational speeds, as discussed in the previous section. Without energy-saving measures, ship operators rely on expanding the fleet. When energy-saving measures are available, the increase in capital costs is more subdued, as a smaller portion of the capital is allocated to fleet expansion. A portion of capital expenditure in this scenario is directed toward investments in energy-saving technologies, which require upfront costs but help maintain overall operational efficiency.

In both scenarios, voyage costs see only a modest increase as carbon prices rise (see figure 10-11). This is primarily due to reduced fuel consumption, which offsets the rising carbon costs. As vessel speeds decrease and EM are implemented, fuel consumption declines, resulting in lower overall fuel costs. Consequently, we observe an asymptotic trend in the carbon-related portion of voyage costs (see figure 12-13), indicating that the carbon price impact is partially absorbed by reduced fuel consumption. In contrast, capital expenditures increase significantly, especially when EM are not available. This surge is driven by the need for more vessels to compensate for slower operational speeds, as discussed previously. Without EM, ship operators expand their fleets. When such measures are available, the rise in capital costs is less pronounced, as funds are allocated to energy-saving technologies that, despite requiring upfront investment, help maintain operational efficiency.

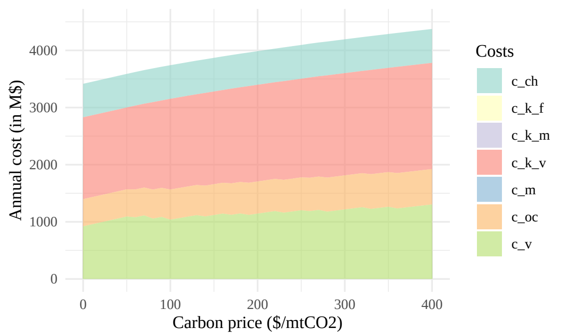

Figure 10: Share of costs without energy savings, under a carbon tax of 0-400$/mtCO2

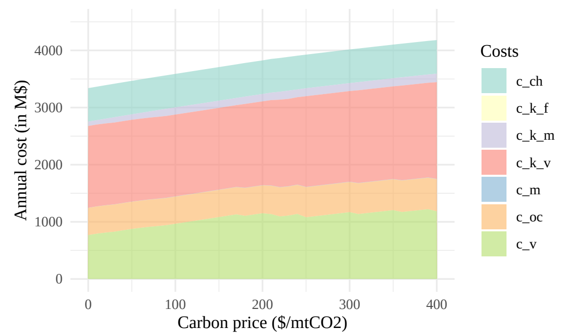

Figure 11: Share of costs with energy savings, under a carbon tax of 0-400$/mtCO2

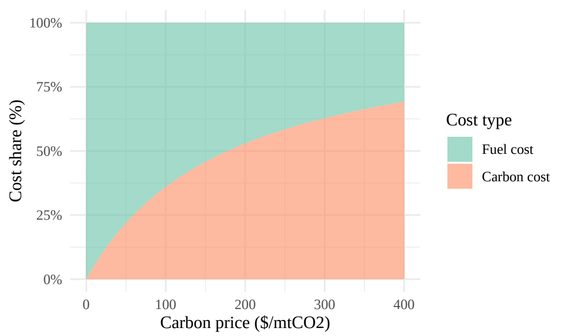

Figure 12: Share of fuel cost without energy savings, under a carbon tax of 0-400$/mtCO2

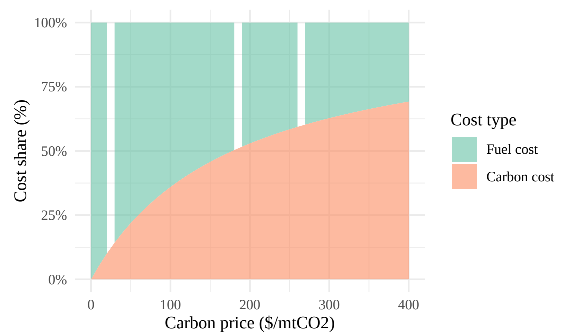

Figure 13: Share of fuel cost with energy savings, under a carbon tax of 0-400$/mtCO2

Comparing the total costs across both scenarios, we observe that even in the absence of a carbon price, the scenario with energy-saving measures incurs lower costs. This is due to the installation of measures that are already cost-effective without the need for carbon pricing. These technologies are considered to have a negative marginal abatement cost, meaning they generate net savings by reducing fuel consumption and emissions while lowering overall operational costs. At the highest carbon price level of $400 per tonne, the total cost difference between the two scenarios narrows to 4%.

5.4 Carbon emissions and measures

Without EM, carbon emissions are primarily reduced by lowering vessel speed. As carbon prices increase, emissions decrease gradually in line with the reduction in speed. However, with the availability of EM, emissions decline steadily due to investments in these technologies, allowing reductions without requiring immediate operational changes. Up to a carbon price of \$100 per tonne, emissions are continuously reduced through technological improvements alone. At more than 100\$/mtCO2, carbon emissions of each scenario converge to a point where current measures are no longer adequate to achieve further reductions. This indicates that within this price range, the most energy efficient combination of EM is achieved, maximizing emissions reductions. Beyond this threshold, further decarbonization from these measures stops and then operational measures take the lead. Thanks to previous investment, every ship benefit from energy efficient technologies so emissions stay lower than in the no-EM scenario.

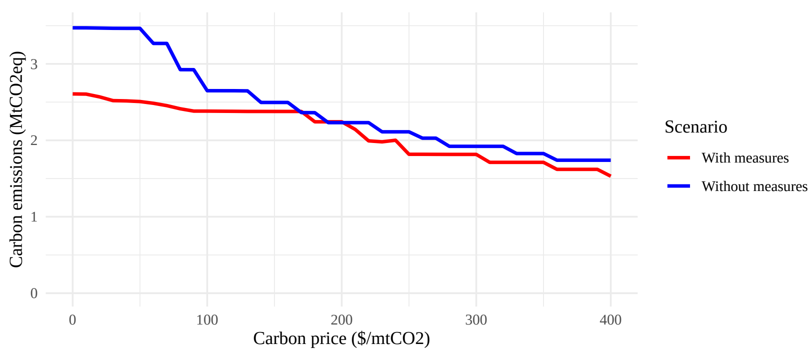

Figure 14: Carbon emissions by scenario without ETS zone, under a carbon tax of 0-400\$/mtCO2

Figure 15 illustrates this phenomenon: emissions for a large ship remain stagnant between \$100/tCO2 and \$150/mtCO2, reflecting the halt in further investment. Emissions only start decreasing again when vessel speed is reduced.

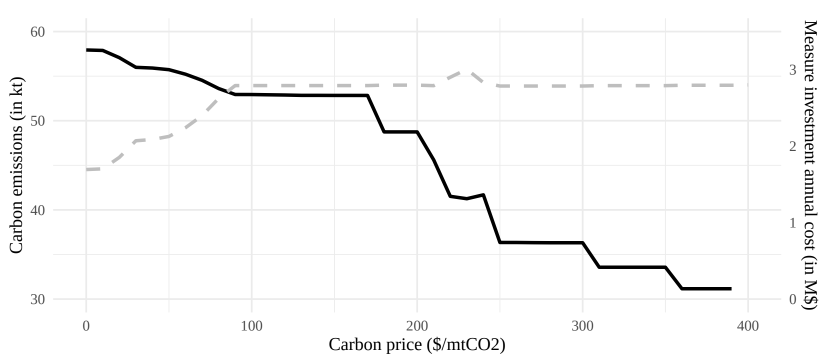

Figure 15: Annual carbon emissions and investment cost in measures for one single large vessel, under a carbon tax of 0-400\$/mtCO2

5.5 Fuel switch

With carbon prices ranging from \$0 to \$400 per tonne, no fuel switching occurs due to the high investment costs required. The carbon price is insufficient to justify the expense of adopting alternative fuels. Higher carbon price simulations would be needed to trigger this kind of adaptation.

6 Conclusion

Our simulations reveal that while the implementation of carbon taxes yields significant reductions in emissions, these reductions alone are insufficient to meet full decarbonization goals. Energy-saving measures (EM) play a crucial role under low carbon prices. These measures help reduce emissions without the need for drastic reductions in vessel speeds, which is critical for maintaining operational efficiency and service levels in maritime shipping. However, these measures alone are not enough to fully decarbonize the sector. Furthermore, the expansion of the ship fleet can be viewed as a form of carbon leakage, as it effectively shifts emissions from operational activities to those linked with the construction and sale of new ships. Accurately assessing this impact would necessitate a comprehensive life cycle analysis.

To achieve complete decarbonization, the transition to alternative fuels is essential. Unfortunately, alternative fuels are not yet economically viable under current carbon pricing levels (especially the actual under 100$ 2024 EU ETS price) . They will only become competitive when carbon prices reach significantly higher levels. This highlights the necessity of public investment in the development and deployment of alternative fuel technologies. Additionally, further investment in energy efficiency research is needed to reduce energy cost.

References

Adland, R., Cariou, P., and Wolff, F.-C. (2020). Optimal ship speed and the cubic law revisited: Empirical evidence from an oil tanker fleet. *Transportation Research Part E: Logistics and Transportation Review*, 140:101972.

Brynolf, S. (2014). Environmental assessment of present and future marine fuels. *Chalmers University of Technology.*

Cariou, P. (2011). Is slow steaming a sustainable means of reducing co2 emissions from container shipping? *Transportation Research Part D: Transport and Environment*, 16(3):260–264.

Cariou, P., Halim, R. A., and Rickard, B. J. (2023). Ship-owner response to carbon taxes: Industry and environmental implications. *Ecological Economics*, 212:107917.

Cariou, P., Parola, F., and Notteboom, T. (2019). Towards low carbon global supply chains: A multi-trade analysis of co2 emission reductions in container shipping. *International Journal of Production Economics*, 208:17–28.

Cepeda, M. A. F., Assis, L. F., Marujo, L. G., and Caprace, J.-D. (2017). Effects of slow steaming strategies on a ship fleet. *Marine Systems & Ocean Technology*, 12(3):178–186.

Comer, B. and Osipova, L. (2021). Accounting for well-to-wake carbon dioxide equivalent emissions in maritime transportation climate policies.

Corbett, J. J., Wang, H., and Winebrake, J. J. (2009). The effectiveness and costs of speed reductions on emissions from international shipping. *Transportation Research Part D: Transport and Environment*, 14(8):593–598.

Dinu, O. and Ilie, A. (2015). Maritime vessel obsolescence, life cycle cost and design service life. In *IOP conference series: materials science and engineering*, volume 95, page 012067. IOP Publishing.

EU Council (2023). Fueleu maritime initiative: Council adopts new law to decarbonise the maritime sector - consilium.

Faber, J., Hanayama, S., Zhang, S., and Pereda, P. (2021). Fourth imo greenhouse gas study. Technical Report 4, International Maritime Organization, London.

Faber, J., Wang, H., Nelissen, D., Russell, B., and St Amand, D. (2011). Marginal abatement costs and cost effectiveness of energy-efficiency measures. MARINE ENVIRONMENT PROTECTION COMMITTEE, 62nd session, Agenda item 5, MEPC 62/INF.7, 8 April 2011, ENGLISH ONLY.

Gelareh, S. and Meng, Q. (2010). A novel modeling approach for the fleet deployment problem within a short-term planning horizon. *Transportation Research Part E: Logistics and Transportation Review*, 46(1):76–89.

Grahn, M., Taljegard, M., and Bengtsson, S. (2013). Cost-effective choices of marine fuels under stringent carbon dioxide targets. *Conference Proceedings.*

Gu, Y., Wallace, S. W., and Wang, X. (2019). Can an emission trading scheme really reduce co2 emissions in the short term? evidence from a maritime fleet composition and deployment model. *Transportation Research Part D: Transport and Environment*, 74:318–338.

Gundersen, H. and S. Elde, M. (2016). Project report - ee appraisal tool for imo. *International Maritime Organization.*

Herrera Rodriguez, M., Agrell, P. J., Manrique-de Lara-Peñate, C., and Trujillo, L. (2022). A multi-criteria fleet deployment model for cost, time and environmental impact. *International Journal of Production Economics*, 243:108325.

IHS (2015). *IHS Fairplay World Shipping Encyclopedia*. IHS Fairplay.

IMO (2024). Improving the energy efficiency of ships.

Irena, K., Ernst, W., and Alexandros, C. G. (2021). The cost-effectiveness of co2 mitigation measures for the decarbonisation of shipping. the case study of a globally operating ship-management company. *Journal of Cleaner Production*, 316:128094.

Jaramillo, D. I. and Perakis, A. N. (1991). Fleet deployment optimization for liner shipping part 2. implementation and results. *Maritime Policy & Management*, 18(4):235–262.

Kesicki, F. and Ekins, P. (2012). Marginal abatement cost curves: a call for caution. *Climate Policy*, 12(2):219–236.

Kontovas, C. A. (2014). The green ship routing and scheduling problem (gsrsp): A conceptual approach. *Transportation Research Part D: Transport and Environment*, 31:61–69.

Kristensen, H. O. H. (2012). Model for environmental assessment of container ship transport: Sname annual meeting. *Society of Naval Architects and Marine Engineers. Transactions*, 118:122–139.

Lindstad, H., Asbjørnslett, B. E., and Strømman, A. H. (2011). Reductions in greenhouse gas emissions and cost by shipping at lower speeds. *Energy Policy*, 39(6):3456–3464.

Lindstad, H., Verbeek, R., Blok, M., van Zyl, S., Hübscher, A., Kramer, H., Purwanto, J., Ivanova, O., Boonman, H., and TNO (2015). Ghg emission reduction potential of eu-related maritime transport and on its impacts. *TNO*.

MAN Energy Solutions (2024). Propulsion trends in container vessels. Whitepaper.

Murray, W. (2016). Economies of scale in container ship costs. *United States Merchant Marine Academy*.

Møller, K. T., Jensen, T. R., Akiba, E., and Li, H.-w. (2017). Hydrogen - a sustainable energy carrier. *Progress in Natural Science: Materials International*, 27(1):34–40.

Nepomuceno de Oliveira, M. A., Szklo, A., and Castelo Branco, D. A. (2022). Implementation of maritime transport mitigation measures according to their marginal abatement costs and their mitigation potentials. *Energy Policy*, 160:112699.

Norlund, E. K. and Gribkovskaia, I. (2013). Reducing emissions through speed optimization in supply vessel operations. *Transportation Research Part D: Transport and Environment*, 23:105–113.

Notteboom, T. and Cariou, P. (2009). Fuel surcharge practices of container shipping lines: Is it about cost recovery or revenue-making. page 24–26.

OECD (2022). Ocean shipping and shipbuilding.

OECD (2023). New estimates provide insights on co2 emissions from global shipping.

Perakis, A. N. and Jaramillo, D. I. (1991). Fleet deployment optimization for liner shipping part 1. background, problem formulation and solution approaches. *Maritime Policy & Management*, 18(3):183–200.

Psaraftis, H. N. and Kontovas, C. A. (2010). Balancing the economic and environmental performance of maritime transportation. *Transportation Research Part D: Transport and Environment*, 15(8):458–462.

Ren, J. and Lützen, M. (2015). Fuzzy multi-criteria decision-making method for technology selection for emissions reduction from shipping under uncertainties. *Transportation Research Part D: Transport and Environment*, 40:43–60.

Schwartz, H., Gustafsson, M., and Spohr, J. (2020). Emission abatement in shipping – is it possible to reduce carbon dioxide emissions profitably? *Journal of Cleaner Production*, 254:120069.

Shintani, K., Imai, A., Nishimura, E., and Papadimitriou, S. (2007). The container shipping network design problem with empty container repositioning. *Transportation Research Part E: Logistics and Transportation Review*, 43(1):39–59.

Stopford, M. (2010). *Maritime economics*. Routledge, London, 3. ed., repr edition.

Taskar, B. and Andersen, P. (2020). Benefit of speed reduction for ships in different weather conditions. *Transportation Research Part D: Transport and Environment*, 85:102337.

Tran, N. K. and Lam, J. S. L. (2022). Effects of container ship speed on co2 emission, cargo lead time and supply chain costs. *Research in Transportation Business & Management*, 43:100723.

UNCTAD (2023). Review of maritime transport 2023. Technical report, UNCTAD.

Wang, K., Fu, X., and Luo, M. (2015). Modeling the impacts of alternative emission trading schemes on international shipping. *Transportation Research Part A: Policy and Practice*, 77:35–49.

Wang, S. and Meng, Q. (2012). Liner ship fleet deployment with container transshipment operations. *Transportation Research Part E: Logistics and Transportation Review*, 48(2):470–484.

Wang, S. and Meng, Q. (2017). Container liner fleet deployment: A systematic overview. *Transportation Research Part C: Emerging Technologies*, 77:389–404.

Woo, J.-K. and Moon, D. S.-H. (2014). The effects of slow steaming on the environmental performance in liner shipping. *Maritime Policy & Management*, 41(2):176–191.

Xia, J., Li, K. X., Ma, H., and Xu, Z. (2015). Joint planning of fleet deployment, speed optimization, and cargo allocation for liner shipping. *Transportation Science*, 49(4):922–938.

Yuan, J., Ng, S. H., and Sou, W. S. (2016). Uncertainty quantification of co2 emission reduction for maritime shipping. *Energy Policy*, 88:113–130.

Zhen, L., Wu, Y., Wang, S., and Laporte, G. (2020). Green technology adoption for fleet deployment in a shipping network. *Transportation Research Part B: Methodological*, 139:388–410.

Zhu, M., Yuen, K. F., Ge, J. W., and Li, K. X. (2018). Impact of maritime emissions trading system on fleet deployment and mitigation of co2 emission. *Transportation Research Part D: Transport and Environment*, 62:474–488.

A Routes data

Ports	Distance (nm)
Busan, KR ⟶ Ningbo, CN	512
Ningbo, CN ⟶ Shanghai, CN	51
Shanghai, CN ⟶ Yantian, CN	787
Yantian, CN ⟶ Singapore	1455
Singapore ⟶ Le Havre, FR	8263
Le Havre, FR ⟶ Dunkirk, FR	163
Dunkirk, FR ⟶ Hamburg, FR	421
Hamburg, FR ⟶ Gdansk, PL	483
Gdansk, PL ⟶ Rotterdam, NL	710
Rotterdam, NL ⟶ Jeddah, SA	4075
Jeddah, SA ⟶ Port Klang, MY	4195
Port Klang, MY ⟶ Busan, KT	2719

Ports	Distance (nm)
Qingdao, CN ⟶ Shanghai, CN	380
Shanghai, CN ⟶ Ningbo, CN	51
Ningbo, CN ⟶ Yantian, CN	747
Yantian, CN ⟶ Singapore, SG	1455
Singapore, SG ⟶ Tanger Med, MA	7036
Tanger Med, MA ⟶ Rotterdam, NL	1404
Rotterdam, NL ⟶ Southampton, GB	255
Southampton, GB ⟶ Antwerp, BE	263
Antwerp, BE ⟶ Le Havre, FR	245
Le Havre, FR ⟶ Algeciras, ES	1263
Algeciras, ES ⟶ Qingdao, CN	9475

Ports	Distance (nm)
Jebel Ali, AE ⟶ Khalifa, UAE	50
Khalifa, UAE ⟶ Karachi, PK	777
Karachi, PK ⟶ Nhava Sheva, IN	524
Nhava Sheva, IN ⟶ Mundra, IN	403
Mundra, IN ⟶ Jeddah, SA	2300
Jeddah, SA ⟶ Malta	1673
Malta ⟶ Tanger Med, MA	1016
Tanger Med, MA ⟶ Southampton, GB	1205
Southampton, GB ⟶ Rotterdam, NL	263
Rotterdam, NL ⟶ Bremerhaven, DE	277
Bremerhaven, DE ⟶ Antwerp, BE	357
Antwerp, BE ⟶ Dunkirk, FR	94
Dunkirk, FR ⟶ Le Havre, FR	155
Le Havre, FR ⟶ Algeciras, ES	1263
Algeciras, ES ⟶ Jebel Ali, AE	4927

Table 9: FAL1, FAL3 and EPIC routes

Ports	Distance (nm)
Shanghai, CN ⟶ Ningbo, CN	51
Ningbo, CN ⟶ Xiamen, CN	500
Xiamen, CN ⟶ Shekou, CN	336
Shekou, CN ⟶ Singapore, SG	1431
Singapore, SG ⟶ Alexandria, EG	5273
Alexandria, EG ⟶ Beirut, LB	346
Beirut, LB ⟶ Tripoli, LB	57
Tripoli, LB ⟶ Izmit, TR	922
Izmit, TR ⟶ Istanbul, TR	43
Istanbul, TR ⟶ Constanta, RO	196
Constanta, RO ⟶ Piraeus, GR	556
Piraeus, GR ⟶ Jeddah, SA	1335
Jeddah, SA ⟶ Port Klang, MY	4195
Port Klang, MY ⟶ Shanghai, CN	2341

Ports	Distance (nm)
Shanghai, CN ⟶ Ningbo, CN	51
Ningbo, CN ⟶ Busan, KR	512
Busan, KR ⟶ Shekou, CN	1188
Shekou, CN ⟶ Singapore, SG	1431
Singapore, SG ⟶ Alexandria, EG	5273
Alexandria, EG ⟶ Koper, SI	1245
Koper, SI ⟶ Trieste, IT	6
Trieste, IT ⟶ Rijeka, HR	150
Rijeka, HR ⟶ Port Said, EG	1315
Port Said, EG ⟶ Jeddah, SA	717
Jeddah, SA ⟶ Port Klang, MY	4195
Port Klang, MY ⟶ Shanghai, CN	2230

Ports	Distance (nm)
Qingdao, CN ⟶ Busan, KR	525
Busan, KR ⟶ Shanghai, CN	467
Shanghai, CN ⟶ Ningbo, CN	51
Ningbo, CN ⟶ Xiamen, CN	500
Xiamen, CN ⟶ Nansha, CN	352
Nansha, CN ⟶ Shekou, CN	21
Shekou, CN ⟶ Singapore, SG	1431
Singapore, SG ⟶ Malta	6041
Malta ⟶ Valencia, ES	768
Valencia, ES ⟶ Barcelona, ES	170
Barcelona, ES ⟶ Fos-sur-Mer, FR	208
Fos-sur-Mer, FR ⟶ Genoa, IT	253
Genoa, IT ⟶ Beirut, LN	1540
Beirut, LN ⟶ Jeddah, SA	960
Jeddah, SA ⟶ Jebel Ali, UAE	2310
Jebel Ali, UAE ⟶ Port Klang, MY	3322
Port Klang, MY ⟶ Qingdao, CN	2686

Table 10: BEX, BEX2 and MEX routes

B Measures data

To make our model work, we need energy saving measures data as consumption reduction potential, annual recuring costs and investment costs for 8000, 12000 and 18000 TEU containerships vessels. There is a technical literature that compiles these data but this is limited to certain type of vessels and capacities. As we focus on containerships, we only keep these vessel-type specific data. Using simple data processing methods, we have tried to homogenise the data in order to obtain consistent results.

We use data from 5 main sources :

- Faber et al. (2011) : Data from several technical sources and direct interviews of operators and others with experience with the measures
- Lindstad et al. (2015) : Data from several technical sources
- Gundersen and S. Elde (2016) : Data from DNV GL R&D projects and experience gained from energy efficiency studies involving 25+ customers operating 900+ ships
- Irena et al. (2021) : Data from a "desk-research or consultation with industry experts"
- Faber et al. (2021) : Data from several sources

From Faber et al. (2021), we obtain a list of measures including energy-saving technologies, use of renewable energy, use of alternative fuels and speed reduction. This list set the base of measures available in our model. According to Irena et al. (2021), some measures are highly correlated, so combining them doesn't provide extra savings, leading to potential double-counting. To address this, the IMO has grouped these measures, allowing only one to be selected from each group. As IMO also based its work on literature data, they propose an extrapolation method based either on engine power or ship size depending on measure type. The full measure list is available in table 12. For these 44 measures we have:

- Type of measure (energy-saving technologies, renewable energy, alternative fuels, speed reduction)
- Group of technologies
- Category of maturity between 1 and 4
  - 1 : Matured and available on the market for < 5 years
  - 2 : Matured and available on the market for = < 5 years
  - 3 : Evolving, with some units available
  - 4 : Evolving
- Applicability of technologies
  - 0 : Not applicable for containerships
  - 1 : All ships
  - 2 : Only new ships
- Expected life time or maintenance in years
- Extrapolation method
  - Main engine power in kW
  - Ship size in TEU (Originally in dwt, but TEU is more appropriate for containerships)

Here we focus only on energy-saving measures. From the sources previously cited, we obtain consumption reduction potential, investment and annual recurring cost for different size of containerships vessels. In the table 13 we compile the available data for containerships size by source. Unfortunately, we were not able to find data for every measures[8]. As our vessels size are not represented in data, we extrapolate our data using a (non?) LINEAR model. First, we have to modelize the main engine power depending on vessel size in TEU. For this, using Faber et al. (2021) world fleet data in 2018 (c.f. table 11), we carry out a linear regression by part using mean TEU for explanatory variable and mean kW for dependent variable.

TEU	**kW**
0-999	5077
1000-1999	12083
2000-2999	20630
3000-4999	34559
5000-7999	52566
8000-11999	57901
12000-14499	61231
14500-19999	60202
20000+	60210

Table 11: Average power of main engine in kW according to vessel size in TEU in 2018

Thus, we estimated the main engine power for the specific vessel type for which we have relevant data on emission reduction measures. From our available data we used a simple linear model as equation (58) and (59) with $p^M_{v,m}$ the measure investment cost, kW_v and TEU_v the main engine power and ship size respectively depending on IMO recommended method. We did the same with annual recurring cost. For energy consumption reducing potential, we take the average.

$$p^M_{v,m} = \alpha_m + \beta_m * kW_v \tag{58}$$

$$p^M_{v,m} = \alpha_m + \beta_m * TEU_v \tag{59}$$

The results we obtain are shown in table 15.

[8]Electronic engine control, Steam plant operation improvements, Hull performance monitoring, Hull hydro-blasting, Dry-dock full blast

Measure type	Gr. No.	N°	Measure	Maturity	Applicability	Extrapolation	Lifetime	Code
	Θ_n						n_m	m
(1) Energy-saving technologies	Group 1 Main engine improvements	1	Main Engine Tuning	1	1	kW	25	met
		2	Common-rail	1	1	kW	25	cr
		3	Electronic engine control	1	1	kW	25	eec
	Group 2 Auxiliary systems	4	Frequency converters	1	1	kW	25	fc
		5	Speed control of pumps and fans	1	1	kW	25	scpf
	Group 3 Steam plant	6	Steam plant operation improvements	1	0	kW	25	spoi
	Group 4 Waste heat recovery	7	Waste heat recovery	1	1	kW	25	whr
		8	Exhaust gas boilers on auxiliary engines	1	1	kW	25	egbae
	Group 5 Propeller improvements	9	Propeller-rudder upgrade	1	1	kW	10	pru
		10	Propeller upgrade	1	1	kW	10	pu
		11	Propeller boss cap fins	1	1	kW	10	pbcf
		12	Contra-rotating propeller	1	1	kW	25	crp
	Group 6 Propeller maintenance	13	Propeller performance monitoring	1	1	kW	1	ppm
		14	Propeller polishing	1	1	dwt	1	pp
	Group 7 Air lubrication	15	Air lubrication	2	2	dwt	25	al
	Group 8 Hull coating	16	Low-friction hull coating	1	1	dwt	5	lfhc
	Group 9 Hull maintenance	17	Hull performance monitoring	1	1	dwt	5	hpm
		18	Hull brushing	1	1	dwt	5	hb
		19	Hull hydro-blasting	1	1	dwt	5	hhb
		20	Dry-dock full blast	1	1	dwt	15	ddfb
	Group 10 Optimization of water flow hull openings	21	Optimization water flow hull openings	1	1	dwt	25	owfho
	Group 11 Super light ship	22	Super light ship	3	0	dwt	25	sls
	Group 12 Reduced auxiliary power demand	23	Reduced auxiliary power demand	1	1	kW	25	rapd
(2) Use of renewable energy	Group 13 Wind Power	24	Towing kite	3	2	dwt	25	tk
		25	Wind power (fixed sails or wings)	3	0	kW	25	wp
		26	Wind engine (Flettner rotor)	1	0		25	we
	Group 14 Solar panels	27	Solar panels	3	0		25	sp
(3) Use of alternative fuels	Group 15A Use of alternative fuel with carbons	28	LNG+ICE	3	2	kW	25	lng_ice
		29	LNG+FC	4	2	kW	25	lng_fc
		30	Methanol + ICE	3	2	kW	25	meoh_ice
		31	Ethanol + ICE	4	2	kW	25	eoh_ice
	Group 15B Use of alternative fuel without carbons	32	Hydrogen + ICE or FC	4	2	kW	25	h_ice
		33	Hydrogen + FC	4	2	kW	25	h_fc
		34	Ammonia + ICE	4	2	kW	25	nh3_ice
		35	Ammonia + FC	4	2	kW	25	nh3_fc
		36	Synthetic methane + ICE	4	2	kW	25	sch4_ice
		37	Synthetic methane + FC	4	2	kW	25	scha4_fc
		38	Biomass methane + ICE	4	2	kW	25	bch4_ice
		39	Biomass methane + FC	4	2	kW	25	bch4_fc
		40	Synthetic methanol + ICE	4	2	kW	25	smeoh_ice
		41	Biomass methanol + ICE	4	2	kW	25	bmeoh_ice
		42	Synthetic ethanol + ICE	4	2	kW	25	seoh_ice
		43	Biomass ethanol + ICE	4	2	kW	25	beoh_ice
(4) Speed reduction	Group 16 Speed reduction	44	Speed reduction by 10%	1	1		25	sr1

Table 12: Measures list (Faber et al., 2021)

Measure	Code	Faber et al. (2011)	Lindstad et al. (2015)	Irena et al. (2021)	Gundersen and S. Elde (2016)
Main Engine Tuning	*met*	0 - 8000+		2500 - 8000+	
Common-rail	*cr*	0 - 8000+			
Electronic engine control	*eec*				0 - 8000+
Frequency converters	*fc*			2500 - 8000+	0 - 8000+
Speed control of pumps and fans	*scpf*	0 - 8000+			
Steam plant operation improvements	*spoi*				
Waste heat recovery	*whr*	2000 - 8000+	4000	2500 - 8000+	0 - 8000+
Exhaust gas boilers on auxiliary engines	*egbae*				0 - 8000+
Propeller-rudder upgrade	*pru*	0 - 8000+		2500 - 8000+	
Propeller upgrade (nozzle, tip winglet)	*pu*		4000		0 - 8000+
Propeller boss cap fins	*pbcf*	0 - 8000+		2500 - 8000+	
Contra-rotating propeller	*crp*			2500 - 8000+	0 - 8000+
Propeller performance monitoring	*ppm*			2500 - 8000+	
Propeller polishing	*pp*	0 - 8000+			
Air lubrication	*al*	2000 - 8000+		2500 - 8000+	0 - 8000+
Low-friction hull coating	*lfhc*	0 - 8000+			0 - 8000+
Hull performance monitoring	*hpm*				
Hull brushing	*hb*				
Hull hydro-blasting	*hhb*				
Dry-dock full blast	*ddfb*				
Optimization water flow hull openings	*owfho*	0 - 8000+	4000	2500 - 8000+	
Super light ship	*sls*		4000		
Reduced auxiliary power demand	*rapd*		4000		0 - 8000+

Table 13: Containerships size in TEU available data for energy-saving measures

Measure	Code	Faber et al. (2011)	Lindstad et al. (2015)	Irena et al. (2021)	Gundersen and S. Elde (2016)
Weather routing	wr		4000		0 - 8000+
Autopilot adjustment	aj	0 - 8000+			
Hybridisation	h		4000		
H2 fuel cell for aux power during sailing	h_pe		4000		
Cold ironing	ci		4000	2500 - 8000+	
Voyage Execution	ve			2500 - 8000+	0 - 8000+
Optimization of Trim and Ballast	otb			2500 - 8000+	0 - 8000+
Wake Equalizing Duct	wed			2500 - 8000+	
Carbon Capture for Storage and Sequestration	ccs			2500 - 8000+	
Propulsion Efficiency Devices	ped				0 - 8000+

Table 14: Containerships size in TEU available data for non-IMO-listed energy-saving measures

Measure	**Code**	**Gr. No.**	**N°**	**Reduction potential**	**Investment cost**			**Annual recurring cost**		
				%	*\$2024*			*\$2024*		
	m	Θ_n		τ_m	$P^M_{small,m}$	$P^M_{medium,m}$	$P^M_{large,m}$	$C^M_{small,m}$	$C^M_{medium,m}$	$C^M_{large,m}$
Main Engine Tuning	met	1	1	1.0	800 446	873 061	876 679			
Common-rail	cr	1	2	0.3	324 838	355 144	356 654			
Frequency converters	fc	2	4	10.0	1 700 404	1 802 109	1 807 176	10 842	10 826	10 825
Speed control of pumps and fans	scpf	2	5	0.6	1 882 680	2 049 048	2 057 335	6 650	6 650	6 650
Waste heat recovery	whr	4	7	5.7	12 468 828	13 265 857	13 305 562	38 637	43 755	44 010
Exhaust gas boilers on a-engines	egbae	4	8	5.0	13 198 016	13 608 530	13 628 980	42 031	44 814	44 952
Propeller-rudder upgrade	pru	5	9	4.0	6 151 869	6 721 255	6 749 620	13 300	13 300	13 300
Propeller upgrade	pu	5	10	1.5	1 815 450	1 815 450	1 815 450			
Propeller boss cap fins	pbcf	5	11	2.3	420 095	456 694	458 517			
Contra-rotating propeller	crp	5	12	7.0	3 295 673	3 547 769	3 560 328	38 637	43 437	43 676
Propeller performance monitoring	ppm	6	13	1.0	2 227 667	2 368 310	2 375 316	30 863	31 112	31 125
Propeller polishing	pp	6	14	5.3	210 161	295 602	423 764			
Air lubrication	al	7	15	4.8	2 869 899	3 643 056	4 802 790	12 809	20 578	32 233
Low-friction hull coating	lfhc	8	16	1.9	819 147	1 115 669	1 560 451	13 300	13 300	13 300
Optimization water flow hull openings	owfho	10	21	3.4	384 208	487 467	642 355			
Super light ship	sls	11	22	10.0	4 053 840	4 053 840	4 053 840			
Reduced auxiliary power demand	rapd	12	23	2.4	319 200	319 200	319 200			
Weather routing	wr		46	1.6	159 600	159 600	159 600	1 996	2 187	2 472
Autopilot adjustment	aj		47	1.8	117 758	164 238	233 959	3 990	3 990	3 990
H2 fuel cell for aux power during sailing	h_pe		49	5.0	159 600	159 600	159 600			
Cold ironing	ci		50	68.3	672 453	672 453	672 453			
Voyage Execution	ve		51	1.6	12 809	12 809	12 809	6 440	10 346	16 205
Optimization of Trim and Ballast	otb		52	3.8	18 945	20 068	21 752	6 650	6 650	6 650
Wake Equalizing Duct	wed		53	2.0	103 666	117 670	138 676			
CCS	ccs		54	100.0	801 771	1 263 943	1 957 200	833 281	1 418 315	2 295 867

Table 15: Regression results